Determining the adsorption of dissolved salt from aqueous flow through a packed bed

by

Ruhania Tarannum

B.S., University of Dhaka, Bangladesh, 2011

A THESIS

submitted in partial fulfillment of the
requirements for the degree

MASTER OF SCIENCE

Department of Mechanical and Nuclear Engineering
Carl R. Ice College of Engineering

KANSAS STATE UNIVERSITY
Manhattan, Kansas

2019

Approved by:

Co-Major Professor
Dr. Hitesh Bindra

Approved by:

Co-Major Professor
Dr. William L. Dunn

Copyright

Abstract

Two radio-tracer experiments were designed and performed in the thermal hydraulics laboratory in the Mechanical and Nuclear Engineering Department at Kansas State University. The experiments were intended to reproduce the deposition of dissolved impurities in a debris bed into which salt water had been infused. NaCl and $SrCl_2$ salt containing radioisotopes Na-24 and Sr-85 were used as radio tracers in two experiments to study salt deposition in a tightly packed bed of alumina particles and resin mixture. Color changing cation exchange resin adsorbed the dissolved salt from the injected salt water solution by mutually exchanging corresponding cations. Radiation emitted from the radioactive salt in the bed was detected using a collimated multiple detector system of NaI(Tl) scintillation detectors. The activity and thus the mass of the deposited salt within the interrogated volumes are proportional to the detector response. A Monte Carlo N-Particle (MCNP) model was developed to study the relationship between response and activity/mass. The ultimate purpose was to estimate the build up and retention of tracer within selected regions of the debris bed.

In the first radio tracer experiment, radioactive NaCl salt solution was injected into a packed bed. The gamma rays emitted from the radioactive Na-24 were detected by two NaI(Tl) detectors placed on one side of the packed bed, near the packed bed's top and bottom, respectively. In the second experiment a mixture of radioactive $SrCl_2$ and non-radioactive NaCl salt solution was infused into a packed bed. In this experiment four NaI(Tl) detectors were incorporated in four different locations along the height of the packed bed to detect the gammas emitted by Sr-85. In both experiments, salt solutions were injected at constant flow rate of 10ml/min using an injection pump. All the detectors were placed at the same side of the packed bed and were collimated through lead shields in the two experiments.

Investigating Na-24 tracer experiment and analyzing the detector response data, it was observed that the salt particles mostly adsorbed near the upper portion of the packed bed and almost no salt particles were present in the bottom section of the packed bed. The color change pattern of the resin along the packed bed as well as the radiation counting data of the top and bottom detectors provided the strong evidence of this conclusion. The developed MCNP model resembling the actual experimental set up provided the estimate of the radioactive tracer activity and corresponding detector response. By correlating the simulation results of MCNP model for detector response with the experimental data of radiation detection in Na-24 tracer experiment, it was estimated that approximately $7.41 \pm 0.21pg$ Na-24 was deposited at saturation.In the Sr-85 experiment, it was observed through the resin color change that the salt solution travelled almost all the way through the packed bed system. From the experiment it was estimated that $458.032 \pm 18.68pg$, $79.54 \pm 7.68pg$ and $39.82 \pm 5.4pg$ of Sr-85 were deposited locally within the packed bed in the vicinity of detector-1, detector-2, and detector-4 respectively. Little or no Sr-85 was deposited in the location of the packed bed near detector-3. It is presumed the fact that the packed bed was not formed homogeneously and possibly present a very small amount of resin in the location of packed bed near the detector-3 . It is significant that locations where there is little adsorption of salt can be clearly identified in radio-tracer studies.

Table of Contents

List of Figures . . . viii

List of Tables . . . x

Acknowledgements . . . xi

1 Introduction . . . 1

1.1 Preface . . . 1

1.2 Research Objectives . . . 3

1.3 Design and Methodology . . . 3

2 Literature Review . . . 7

3 Experimental Capabilities and Facilities . . . 13

3.1 TRIGA reactor facility . . . 13

3.2 NaI Scintillation Detector . . . 14

3.3 Electronics for detection system . . . 16

3.3.1 High voltage power supply . . . 16

3.3.2 Preamplifier . . . 17

3.3.3 Amplifier . . . 17

3.3.4 Discriminator . . . 17

3.3.5 Scaler . . . 18

3.3.6 MultiChannel analyzer . . . 18

3.4 NIMbin . . . 18

3.5 Genie-2000 Basic Spectroscopy Software . . . 19

3.6 Lead collimator column . . . 19
3.7 Syringe pump . . . 21
3.8 Conductometer . . . 21
3.9 Fume hood and chemical laboratory facilities . . . 22

4 Design of experiment & MCNP model simulation . . . 24
4.1 Design of the Experiment . . . 24
4.2 Radiotracer Selection . . . 25
4.3 Na-24 Radiotracer Experiment . . . 26
4.3.1 Experimental set up . . . 26
4.3.2 MCNP simulation for design verification . . . 27
4.3.3 Na-24 radiotracer isotope preparation . . . 28
4.3.4 Experimental procedure . . . 28
4.4 Sr-85 Radiotracer Experiment . . . 29
4.4.1 MCNP model development and simulation . . . 29
4.4.2 Detector and collimator set Up . . . 30
4.4.3 Formation of the packed bed . . . 30
4.4.4 Preparation of radioactive salt solution . . . 31
4.4.5 Measurement of conductivity . . . 32
4.4.6 Conduct of the experiment . . . 32
4.4.7 Disposal of radioactive waste . . . 33

5 Results & Discussion . . . 35
5.1 Result analysis of Na-24 radiotracer experiment . . . 35
5.2 Result analysis of Sr-85 radiotracer experiment . . . 39
5.2.1 Salt deposition and color change of packed bed resin . . . 39
5.2.2 Analysis of multiple detector response data . . . 40
5.3 Calculation of local activity and radioactive salt mass deposition . . . 44

5.4 Estimation of the packed bed locations for measured salt deposits 45
5.5 Conclusions 46

Bibliography 48

A Calibration equations for Detectors 51

B MCNP model simulation: Input files 52
B.1 Input file for MCNP model simulation of Na-24 radiotracer experiment . . . 52
B.2 Input file for MCNP model simulation of Sr-85 radiotracer experiment 53

C Activity and mass calculations for local salt deposits 56
C.1 Mass calculation for Na-24 salt deposits in Na-24 radiotracer experiment . . 56
C.2 Activity calculation for locally deposited Sr-85 salt 58
C.3 Mass calculation for the locally deposited Sr-85 salt 59

D Uncertainty calculation 61
D.1 Uncertainty calculation for deposited salt mass in Na-24 radiotracer experiment 61
D.2 Uncertainty calculation for local activity in Sr-85 radiotracer experiment . . 63
D.3 Uncertainty calculation for the mass of Sr-85 deposits in Sr-85 radiotracer experiment 65

List of Figures

1.1 A schematic of the use of a tracer to investigate flow through a system. . . 4

1.2 A drawing of radiotracer experiment to study salt deposition 5

2.1 Radioactivity trace from typical run with flow interruption test 9

2.2 The principle of radiotracer measurement 11

2.3 The principle of adsorption measurement in hydrotransport of solid particles 12

3.1 KSU TRIGA Reactor 14

3.2 NaI(Tl) Scintillation Detector 15

3.3 Detection system 16

3.4 NIMbin 19

3.5 Collimator 20

3.6 Syringe pump 21

3.7 Conductometer 22

3.8 Fumehood and chemical laboratory tools 23

4.1 Design of Sr-85 radiotracer experiment. 26

4.2 Detector-collimator set up for Na-24 radiotracer experiment 27

4.3 Geometry of the MCNP model for the Sr-85 radiotracer experiment. 30

4.4 Collimator-detector set up for Sr-85 radiotracer experiment 31

4.5 Packed bed 32

4.6 Conductivity measurement of salt solution 33

4.7 Disposal of radioactive waste 34

5.1 Resin color change in packed bed due to adsorption of NaCl salt particles in the resin. 36
5.2 Net counts rate Vs time plot for the top detector 37
5.3 Mass deposition over time plot. 39
5.4 Resin color change in packed bed due to salt deposition 40
5.5 Background counts rate for four NaI(Tl) detectors 41
5.6 Detector responses for multiple detector system 42
5.7 Comparison for three detectors net responses 43
5.8 Detector-3 responses for radiation counts and background 44
5.9 Sketch for estimating area for local salt deposition 45

List of Tables

C.1 Detector response data from Sr-85 radiotracer experiment 58

D.1 Top detector response data from Na-24 radiotracer experiment 62

D.2 Detector response data from MCNP simulation 62

Acknowledgments

First, I would like to acknowledge my indebtedness to my major professor Dr. William L. Dunn. I truly consider myself very fortunate for getting the chance to do my master's thesis research work under his supervision. I extend my profound sense of gratitude to Dr. Dunn for his immense support and guidance throughout my research work. This thesis work would not be possible without his expert advice and instructive comments. I owe an inestimable debt to my co-major professor Dr. Hitesh Bindra for giving me the opportunity to join his research lab. It was a unique experience working with him. I am grateful to Dr. Bindra for introducing me to experimental research in a way which made me capable to design and perform experimental works independently. Initially it was difficult for me but at the end I realized this made me more confident and competent embracing and trying new things on my own which I believe a great achievement from this research work and will help me in my future study and career. I would like to express my sincere gratitude to Dr.Steven J. Eckels for advising me as my academic advisor at the beginning of my journey at K-state and guiding me always with his thoughtful suggestions and constructive comments on my research work.

I am thankful to all my colleague from NuEST lab for helping me in various ways during my research work. I express my heartfelt gratitude to my colleague and my first international friend here at KSU, Abhinav Gairola for his untiring support and constant encouragement as a well-wisher and mentor. I am truly thankful to my colleague Zayed Ahmed for always helping me in any kind of need during my whole research period. I am extremely grateful to my colleague Diego Laramore for helping me understanding MCNP model simulations better and patiently responding to my call for help all the time. My special thanks is due to Connor Medlen and Dillon Funk for helping me a lot in building my experimental set up.

I would like to thank my family members and friends who worked as a support system for me in all ups and downs of my academic and personal life in last three years. I could

never thank enough and express my gratitude to my mother, Hafiz Jahan, for what she did for me. It is she who continued to inspire me and support me to accomplish whatever I wished in my life after my father's demise. Her support and inspiration contributed the most in my journey to attain higher education abroad. I should acknowledge my eldest sister, Fahmida Nusrat, for her motivational words and shared views towards life and work which indirectly encouraged me always to keep going and finish my tasks whenever I was stuck with something in my research work. I would love to express my special thanks to my husband, B M Samin Monowar Tonmoy, for his endless support and inspiration. It was never easy for him and me as well, staying thousands of miles apart just after our marriage, for my higher study abroad. I am truly grateful to my husband for understanding me and accepting the emotional struggle and sacrifice with a loving heart. I heartfelt thanks due to my in-laws who have always been my well-wishers and inspired me a lot to pursue my dream of higher education in USA.

I convey my best regards to my all Bangladeshi friends in Manhattan who loved me and supported me always. Grad school is a tough place. Exchanging thoughts and experiences with other grad students really helps to survive better here. I am thankful to everyone who inspired me, supported me and shared thoughts with me in my journey as a grad student at K-state.

Doing master's with thesis research as a graduate student in the department of Mechanical and Nuclear Engineering at Kansas State University has been a tremendous experience of my academic life. I learned a lot in every step I had taken in my graduate research work. That's why, above all, I am grateful to almighty to give me this opportunity of pursuing my higher education in a reputed university of USA and made me capable of completing my master's successfully.

Chapter 1

Introduction

1.1 Preface

Deposition of dissolved and suspended impurities on the process piping is a common phenomena in process industries, manufacturing technologies and in natural aquatic environments. The mechanisms of precipitation and deposition are of significance in chemical, electronic, mineral, biological and environmental industries. These phenomena also play significant roles in the transport of pollutants and geochemical cycling of trace elements in aquatic systems[1]. In different manufacturing and process industries, controlled particle deposition and aggregation is desirable for merchandise fabrication, yet in many other industrial, engineering and reactor processes as well as geochemical and environmental systems deposition is considered as an influence that affects the characteristics and behavior of system operation.

In 2011, the nuclear power industry experienced a disastrous nuclear accident and faced the large challenge to control the damage and catastrophe it caused. The Fukushima Daiichi Nuclear Power Plant (FNPP) lost external power and, due to an earth quake at sea on March 11, 2011, followed by a huge tsunami, lost on-site diesel generator power. The water circulation systems were damaged gravely, and radionuclides were released to the environment for days in the middle of March[2]. In this circumstance, fresh water and sea water were injected by different means to remove the heat[3]. Seawater was injected into the nuclear reactors and

debris bed for long-term cooling. Sea water contains a variety of dissolved salts, minerals and impurities. Injection of sea water was taken as a measure for core cooling during the Fukushima nuclear accident, but the impact of the salt water on the thermal response of the reactor system has not been investigated thoroughly. It is not understood how the dissolved impurities and resulting scale formation affected the coolability. With a goal to understand and model processes such as this, a radiotracer based technique is developed at KSU and benchtop experiments were designed to demonstrate the performance of this technqiue.

Advection, diffusion, retention or resuspension of species as a result of fluid transport in complex heterogeneous media are processes that occur in many nuclear energy related situations. For example, environmental dispersion of radioactive contaminants in the atmosphere, adjacent water bodies or groundwater often has been investigated under accident scenarios or during controlled release of effluents from nuclear facilities[4–7]. Although the effects of effluents may vary in different cases, the dispersal or retention mechanisms in the environment are similar after the release of pollutants, whether radioactive or not. These effluents can be in the form of dissolved or suspended impurities in the discharged fluid stream. Sometimes this is a problem of environmental concern but other times particles can act as tracers to study fluid transport in complex systems[8–10]. In the first case it is important to resolve the dispersal of radioactive elements in the environment and in other scenarios the radioactive species can be used in a time-resolved measurement technique. As an example, radioactive tracers can be used to understand the formation and evolution of scale build-up in process equipment[10].

The objective of this research was to determine research work presented here is aimed at studying local deposition of dissolved salts in an isothermal simulated debris bed. To simulate the local salt deposition in the debris bed, ion-exchange resins are added in the bed that adsorb the salts from an injected radioactive salt solution. The radioisotopes Na-24 and Sr-85 are used as tracers in the salt solution individually in two separate experiments and monitored with detectors placed at different locations along the bed.

1.2 Research Objectives

The objective of this research was to determine the spatial distribution of salt deposits flowing through a debris bed. The following steps were taken

1. Design radiotracer based experiments that emulate the deposition of dissolved impurities in a debris bed after injection of salt water.

2. Study the correlation of detector response with local activity and corresponding salt deposits using an MCNP model.

3. Incorporate multiple collimated gamma-ray detectors to determine the build-up and retention of tracer within selected regions of the debris bed.

1.3 Design and Methodology

In the present research work, gamma-emitting radiotracers were used to study the deposition of water dissolved salt impurities in a packed bed. A radiotracer or a radioactive label is a chemical compound that contains radioisotope(s) as a constituent. Radioisotopes spontaneously decay and simultaneously emits radiation. Tracing the path of the radiotracer by detection and analysis of the emitted radiation, different process mechanisms such as chemical reaction, deposition, flow visualization, transport kinetics, particle tracking, inter well studies etc, can be explored. Radiotracer technology has been useful and has served as an effective method in industry to diagnose process operation or specific causes of inefficiency in a plant(e.g., Dunn and Davis). This method commonly applied to investigate industrial processes and those environment related systems where a great cost-benefit ratio can be gleaned from process optimization and troubleshooting.

There are several advantages of using radiotracer methods. The radiation emitted by the tracer is easily detectable as well as measurable with high precision.Emitted radiation is independent of pressure, temperature, chemical and physical state.The measured radiation emitting from radiotracer provides direct information regarding the amount of labeled species

and no special model is required to draw conclusion on quantitative analysis. Radiotracers do not affect the chemical and physical properties of the system studied so that the technique can be applied as a non-destructive method[11].

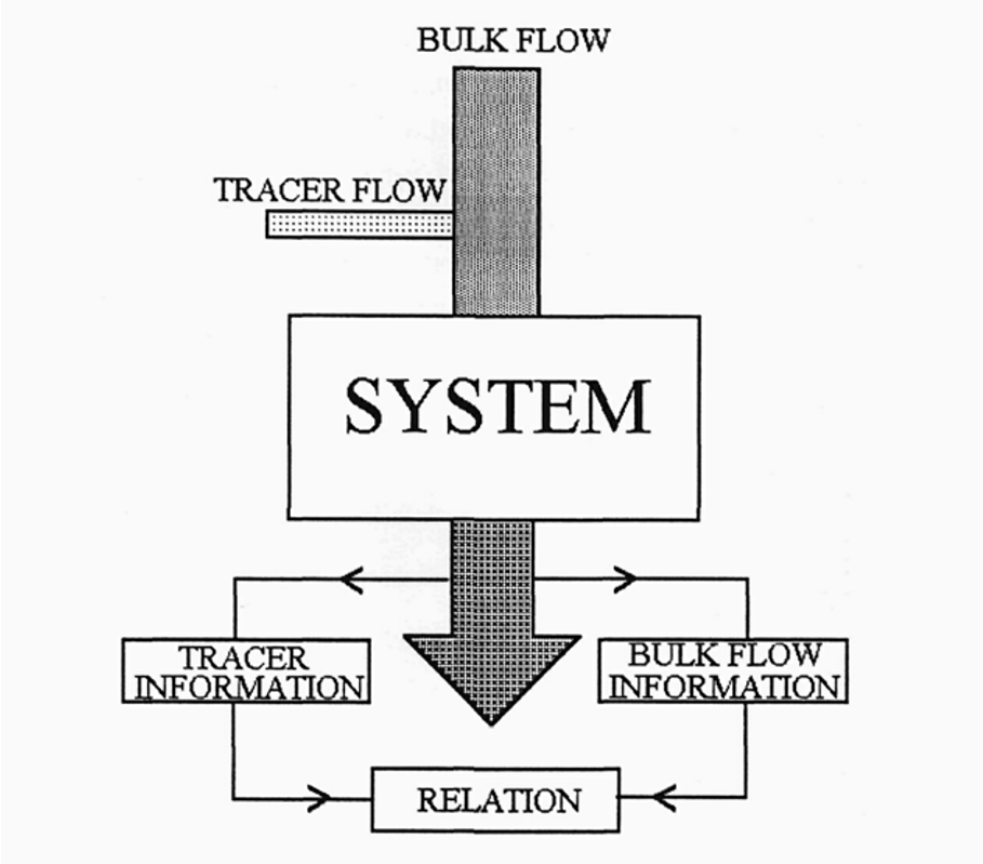

Figure 1.1: A schematic of the use of a tracer to investigate flow through a system.

In general, the tracer can be either radioactive or inert. We consider here the use of radioactive tracers. The general principle of the radiotracer technique (shown in fig. 1.1) is to inject radioactive material which is physio-chemically in similar form of the process material, into the system and monitor the passage of radiotracer along the system at strategically selected locations using radiation detectors.The obtained radiotracer concentration or tracer presence at detection location(s) is plotted as a function of time. In this method hydrodynamic behavior of the process equipment as well as information about occurrence of malfunctions is obtained.[12]

In the present study, two radiotracer experiments were designed in a way that reproduce

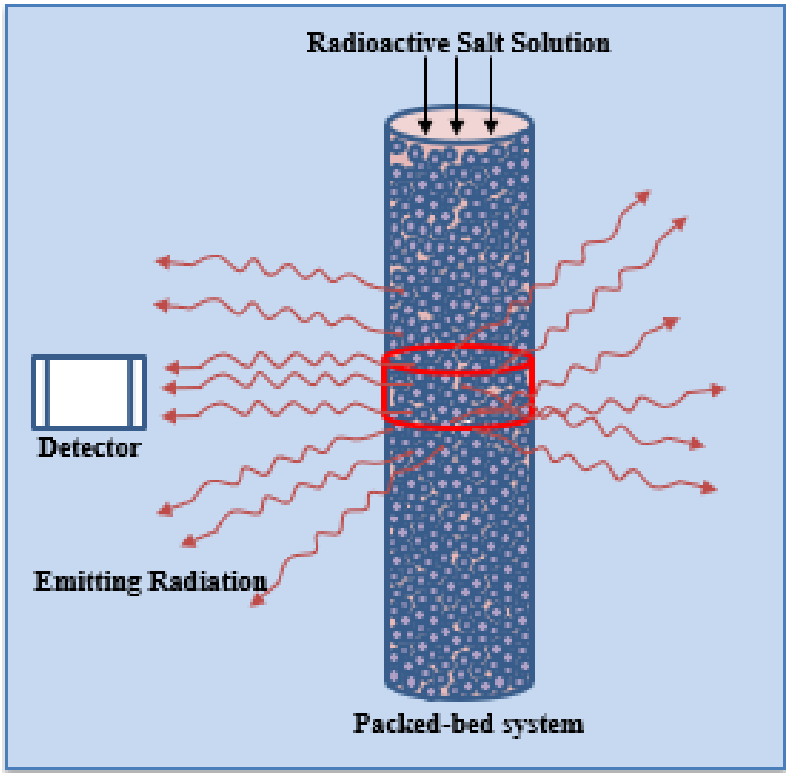

Figure 1.2: Drawing of radiotracer experiment to study salt deposition in packed bed

the deposition of dissolved salt impurities in a debris bed while sea water coolant is injected into the debris bed. To reproduce salt deposition in a debris bed upon injecting sea water coolant, here, in each radiotracer experiment, the packed bed was made of alumina particles, glass particles and resin particles which emulates a debris bed. Sea water contains different minerals and one main salt component of sea water is NaCl. In the first experiment Na-24 radioisotope was used as tracer to study the deposition of NaCl salt in the packed bed by qualitative and quantitative measurements. The radiotracer Na-24 was produced by irradiating NaCl salt in the Kansas State University (KSU) TRIGA reactor facility. An experimental set up was established in the thermal hydraulics lab in the Nuclear Engineering department to facilitate the radiotracer experiment. It was proposed to set up two NaI(Tl) scintillation detectors to detect and analyze radiation emitted from the radioactive salt deposited in two distinct locations of the packed bed. In order to minimize the effect of background counts, a lead collimator column was placed in front of the detector pair to direct the emitted radiation through collimator slits to the detectors. In the second experiment, the

spatial distribution of salt deposits were investigated more rigorously by devising a detector system of four NaI(Tl) detectors at four axial locations of the packed bed. The tracer chosen for this experiment was $SrCl_2$ containing Sr-85 radioisotope.

In radiotracer experiments, after selection of radiotracer, one must estimate the amount of radiotracer required to be used. The acvtivity of the radiotracer is related to the slit size, the detector efficiency and safety considerations. To estimate the amount of the radioactive tracer and corresponding detector response, a monte carlo n-particle (MCNP) model of the experiment was developed. The simulation results of the detector response for the MCNP model was used to correlate the experimental data of detector response with the total deposited activity, which corresponds to the amount of radioactive salt particles deposited in a particular location of the packed bed.

Chapter 2

Literature Review

An ideal tracer behaves exactly like the substance being traced but has some easily distinguished characteristic. Radioisotopes are often nearly ideal tracers because, generally, they behave chemically the same as the nonradioactive isotope, but they emit one or more radiaton particles that can be detected. Gamma-ray-emitting radioisotopes are particularly useful because there are many of them, they are often easily produced, and the gamma rays emitted typically can penetrate many cm of solid or liquid material. In the following, the use of radioisotope tracers will be reviewed and most of the emphasis will be on gamma-emitting radioisotope tracers. Because the use of tracers has been so widespread, the literature review will focus primarily on use of tracers for determining adsorption and deposition in mass flow through media.

Ubiera and Carta conducted radiotracer experiment to investigate protein mass transfer kintics in ion exchange adsorbents for preparative chromatograpy. A trace amount of radioactive I-125 was added to the test protein solution. Labeled Iysozyme test protein solution recirculated through a shallow bed of adsorbent ion-exchange resins. Accumulated radioactivity in column bed was monitored and measured as a function of time with gamma counter. Radioactivity accumulated in the bed was assumed to be proportional to the total adsorbed protein concentration so that the rate of protein mass transfer was measured directly. In the radiotracer mass transfer experiment, at first, radiolabeled protein solution was recirculated

through the empty micro column to get the background due to radioactivity in the protein solution. Next the empty microcolumn was replaced by an identical microcolumn loaded with SP-Sepharose-XL which caused the radioactivity level to drop down to zero. When the radiolabelled protein solution was started to flow through this column, protein adsorption in resin particles caused rapid rise of accumulated radioactivity above the background value. The adsorption slowed down considerably as soon as the flow was stopped. The accumulated radioactivity in microcolumn remained constant since no additional protein solution was fed. After a flow interruption period When the protein solution recirculated through the micro-column again, the protein uptake rate in resin was found faster than just prior to stopping the flow. Uberia and Carta explained this behavior of faster protein uptake in resin as the result of redistribution of protein in particles during flow interruption.The radio-tracer based protein uptake rate in resin was found more precise and in relatively good agreement with measurements carried out with conventional shallow bed method. Two models were considered to fit the data for lysozyme radio-tracer uptake in three different stationary phases with constant diffusivity. The pore diffusion model suit well to fit the protein uptake rate data for SP-sepharose-FF resin, while homogeneous diffusion model appeared more appropriate for SP-sepharose-XL and S-HyperD. But neither model was able to fit uptake rate data in different salt concentration with constant diffusivity. The results appeared were in good qualitative agreement with expected behavior of three different pore structure materials.[13]

Radio tracer technique was applied to study the flow dynamics of heavy petroleum residue in industrial-scale soaker operating in a petroleum refinery.To trace the petroleum residue Bromine-82 as dibromobiphenyl was used as radiotracer. Mean residence time (MRTs) and Residence time distributions (RTD) of residues were measured in this investigation. An axial dispersion model was developed in parallel with tanks-in-series with stagnant volume and exchange to simulate the measured RTD data. The model simulation data fitted very well to the experimentally measure data and identified bypassing or existence two parallel flow paths within the soaker.[14]

A field tracer experiment was performed in the Daejong river of southeast Korea to investigate the process of pollutant transport and to estimate the dispersion coefficient in

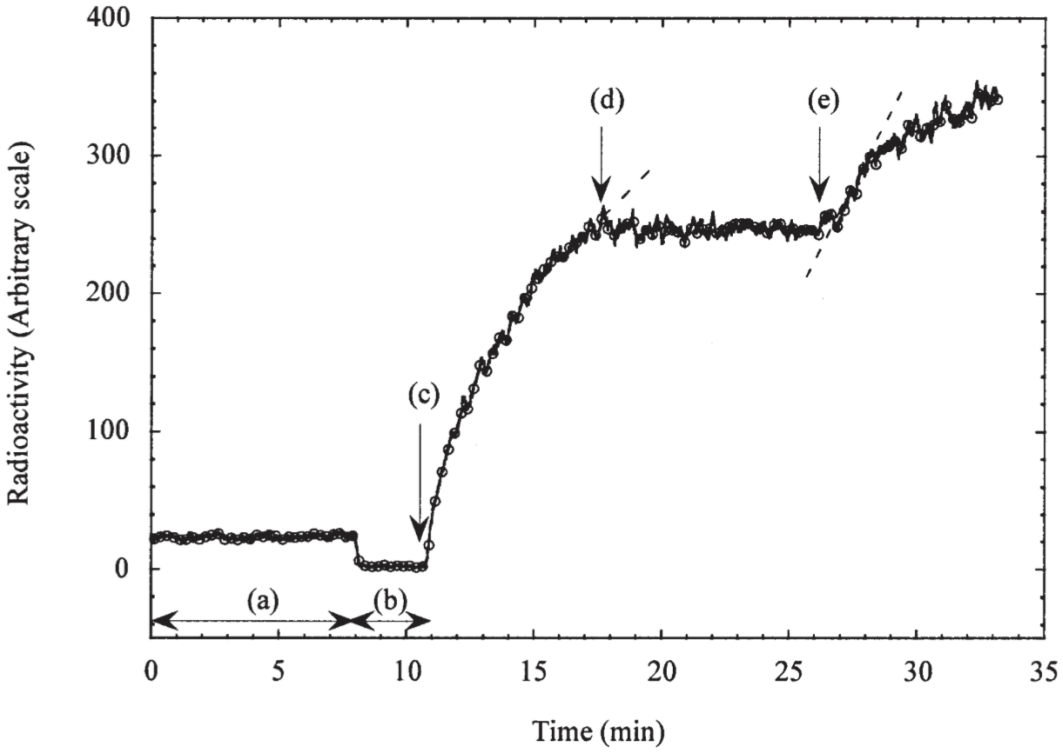

Figure 2.1: Radioactivity trace from typical run with flow interruption test.Period (a): Flow through with empty microcolumn; period (b): empty column replaced with SP-Sepharose-XL microcolumn, no flow; point (c): flow started; point (d) flow stopped; point (e) flow restarted[13]

the river system. A gamma emitting, short-lived radioisotope, Tc-99m (half life 6.02h) was used as trace element and instantaneously injected to the river flow using an underwater glass vial-crusher. The radiation emitting from Tc-99m was detected by two 2" $\times$ 2" NaI(Tl) located at two traverse lines at a downstream position. Multi-channel data acquisition systems were incorporated to process and analyze the detector transmitted signals. In the final results pollutant dispersion coefficient was estimated from radioisotope concentration data[15]

Turner and Smith measured the deposition rate of calcium carbonate on a heat transfer surface using Calcium-47 radio tracer and compared to the measured rate of thermal fouling. They reported the results of an experimental investigation where mass deposition and thermal fouling rates were measured and comparison between the two provided insights into calcium carbonate scaling kinetics. Radiotracer technique was used to determine mass

deposition directly as a function of time through out the fouling experiment. Experiment was carried out in a stainless steel made heat exchanger fouling loop including the test section. The scaling solution containing dissolved Ca-47 radiotracer Experimental results showed the crystalline phase of calcium carbonate that precipitates depends on the degree of supersaturation at heat transfer surface.[16]

In the petroleum industries, enhance oil recovery (EOR) technique is used to increase (average 10%-20%) primary recovery of oil from pores or reservoir rocks. In the petroleum industries, one of the questions of oil-engineers why crude oil comes after water in the gathering stations, though the density of crude oil is lighter than water. The question was tried to be answered by the research work of Sugiharto and his collaborators. Residence time distribution was studied in a multiphase flow system using radiotracer method. I-131 radiotracer was used in the chemical form of Iodo-benzene and sodium Iodide to study the crude oil flow measurement and water flow measurement respectively.From the experimental research it was concluded that water flow is faster than crude oil flow. The probable reason assumed as water in water domain system serves a carrier that carrying crude oil between the layer of water and gas flows. Estimated model parameter from tank-in-series model showed there was relatively high degree of mixing. A rough estimation of Reynolds number showed the water is turbulant in character.[17]

Sorption and desorption characteristics of Zn(II) on the surface soils near nuclear plant sites using radiotracer technique was studied in India. Bulk surface soil samples were collected from three different nuclear power plant sites. Soil samples were processed and analyzed for physi-ochemical properties. Zn-65 was procured and used as radiotracer for the experiment to investigate Z(II) adsorption in soil.[18]

Hydrotransport of solid particles (ceramic models of polymetallic nodules) in a vertical pipeline was studied using radioisotope methods: tracer method and gamma adsorption. In this research work radiotracer method was applied to determine the velocity of selected solid particles representing specified size fraction while gamma adsorption technique was used to measure the mean transport velocity of entire dispersed phase. It is shown through the experimental data analysis that different fraction of solid particles have moved with different

velocities having the same flow velocity of water. The lowest velocities were determined for the particles with largest diameters. Measurements of the radioisotope methods were performed by NaI(Tl) scintillation detectors.

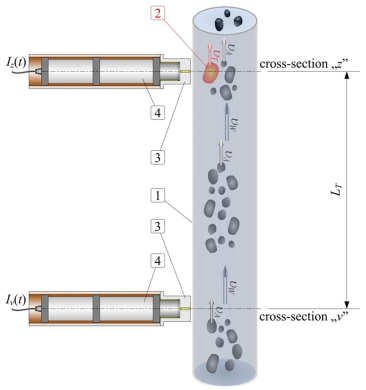

Figure 2.2: The principle of radiotracer measurement: 1 – pipeline with a flowing mixture, 2 – grain marked with a gamma-emitting isotope, 3 – probe collimator, 4 – scintillation detector; LT – distance between sections "v" and "z"; $I_v(t)$, $I_z(t)$ – signals from probes; v_A – mean velocity of solid phase, v_W – velocity of water, v_T – velocity of marked grain.[19]

In the radiotracer experiment to study solid particle velocity, a grain of selected size was radio-isotope marked and introduced into the two phase flow with other unmarked ceramic models. TcO2 containing the Tc-99m radioisotope was inserted into the bores drilled in the selected grain for the isotope-marking. During the flow, marked grain generated signals in two spatially distributed NaI(Ti) detectors.

In gamma adsorption experiment two photo beams, emitted from two sealed Am-241 linear sources, passed through the flowing two-phase mixture. The photo beams were partially adsorbed by the two-phase mixture and detected by two NaI(Tl) detectors in collomators. For both radiotracer method and adsorption method, corresponding mean transportation time delay of single marked grain and two-phase mixture grains were calculated using cross-correlation function (CCF) of the experimental counting data.It was assumed that the most probable transportation time delay of solid phase is expressed by the argument of the main CCF maximum. Grain velocities from tracer experiment and mean velocity of grains finally determined from mean transportation time delay and spatial distance between detectors in each case of both radiometric experiments.[19]

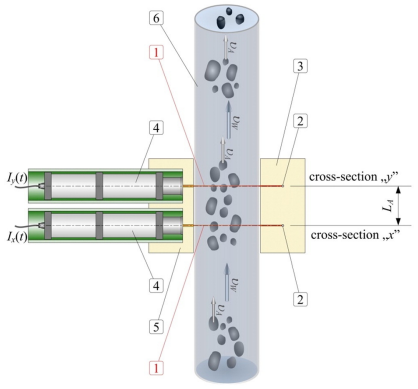

Figure 2.3: The principle of adsorption measurement in hydrotransport of solid particles: 1 – gamma-ray beam, 2 – sealed linear source, 3 – collimator of sources, 4 – scintillation probe, 5 – collimator of detectors, 6 – pipeline with the mixture; LA – distance between sections "x" and "y"; $I_x(t)$, $I_y(t)$ – signals from detectors, v_A – mean velocity of solid phase, v_W – water velocity.[19]

Radiotracer technique has been used from the last century to study different aspects of research fields. This method has been developed and implemented to investigate particle tracking, flow kintetics, transport phenomena of particles,adsorption and desorption of specific materials. salt deposition study in packed bed by designing a radio-tracer based experiment is a new approach to investigate deposits spatial distribution in a debris bed like medium.

Chapter 3

Experimental Capabilities and Facilities

3.1 TRIGA reactor facility

Kansas State University operates a TRIGA MARK II research reactor. The maximum operational power of the reactor is licensed to be $1.25MW$. The TRIGA reactor on campus is equipped with in-core and ex-core irradiation facilities. The in-core and in-pool irradiation facilities include a well in the reflector around the core, the central thimble, the pool iteself, and small penetrations in the upper grid plate that permit small samples to be placed within spaces between fuel elements. Ex-core irradiation facilities include beam tubes that extend radially or tangentially from the core to the experiment floor surrounding the reactor shielding, a section of graphite accessible from the experiment floor, and a section of graphite accessible under water.

The KSU TRIGA reactor is a water moderated, water-cooled thermal reactor. The reactor core consists of 81 fuel elements typically and the heterogeneous fuel elements of the reactor normally consist of 20% enriched uranium in a zirconium hydride matrix and clad with stainless steel.

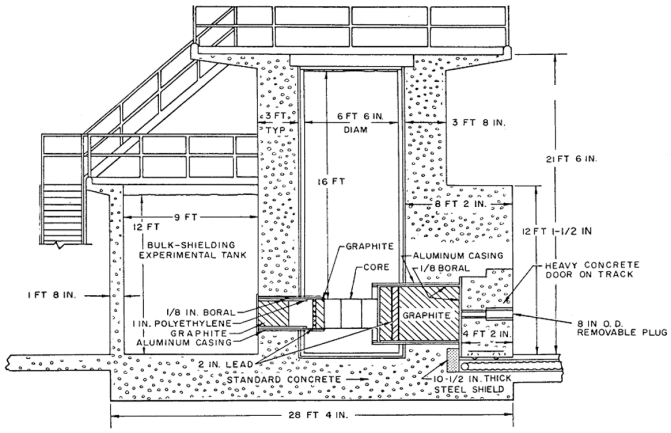

(a) Vertical section through the KSU TRIGA reactor

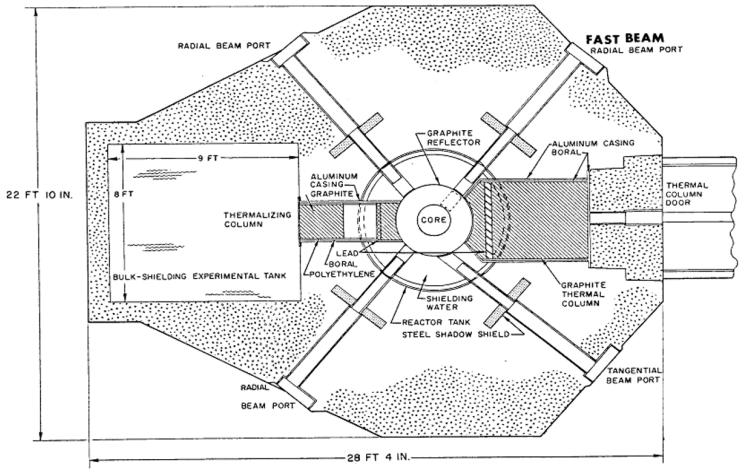

(b) Horizontal section through the KSU TRIGA reactor

Figure 3.1: KSU TRIGA Reactor

3.2 NaI Scintillation Detector

In the present research work, multiple detectors are used to study the spatial distribution of radiotracer-tagged salt deposits in packed beds. Up to four 3" $\times$ 3" NaI(Tl) scintillation detectors are arrangd in a collimated system to detect the gamma radiation emitted from the radioactive salt deposits. NaI(Tl) detectors are widely used gamma detectors in radiotracer applications. NaI(Tl) crystals are inorganic scintillators, activated with thallium as an impurity. NaI crystals are hygroscopic and thus when used for radiation detection they should be sealed hermetically. The emission spectrum of NaI(Tl) peaks at $410nm$ and its light-conversion efficiency is the highest among all inorganic scintillators.

Figure 3.2: NaI(Tl) Scintillation Detector

Most NaI(Tl) detectors have two main components: the NaI(Tl) inorganic crystal and a photomultiplier tube. There are two broad steps in the operation of any scintillation detector. The first step is scintillation in which radiation energy is adsorbed by the scintillator (NaI crystal) and photons are produced in visible or near-visible part of the electromagnetic spectrum. In the second step light is amplified by a photomultiplier tube and and an output pulse is produced.[20]

The scintillation process in inorganic scintillator crystals like NaI(Tl) is best explained by electron-band theory. In pure NaI crystal electrons exist in two energy bands: conduction band and valence band. All electrons remain in the valance band when the crystal is in the ground state. Due to interaction with radiation, some electrons can get excited from the valence to the conduction band, where they can freely migrate within the lattice. When an electron returns to the ground state or valance band from the excited state or conduction band, it can emit a photon. This emitted photon has the characteristic energy equal to the energy gap between valence band and conduction bands. The released photon has the resonance energy and again gets adsorbed by another electron in valence band and raises it back to the conduction band. Therefore in this scintillation process within pure NaI crystals, emitted photons go through resonance adsorption by the crystal itself. Because there are

alternate mechanisms of energy transfer, sometimes excited electrons return back to the ground state by the emission of heat rather than a resonance photon.[21]

Impurities are added to the inorganic scintillator to increase the probability of the visible photon emission during the de-excitation process of electrons. These impurities, called activators, offer sites in the lattice so that new energy states created in between the valence band and the conduction band. These energy states allow electrons to raise to a state with energy less than the conduction band energy. As the energy is less than that of the full forbidden energy gap (energy difference between valence band and conduction band), de-excitation of electron this time can give rise to a photon at visible energy spectrum and therefore serve as the basis of the scintillation process.[22]

A photomultiplier tube often is an integral part of a scintillation detection system that acts as a fast amplifier and amplifies the photoelectrons formed by adsorption of the visible photons in a photo-cathode into an electrical pulse in times of the order of a nanosecond.

3.3 Electronics for detection system

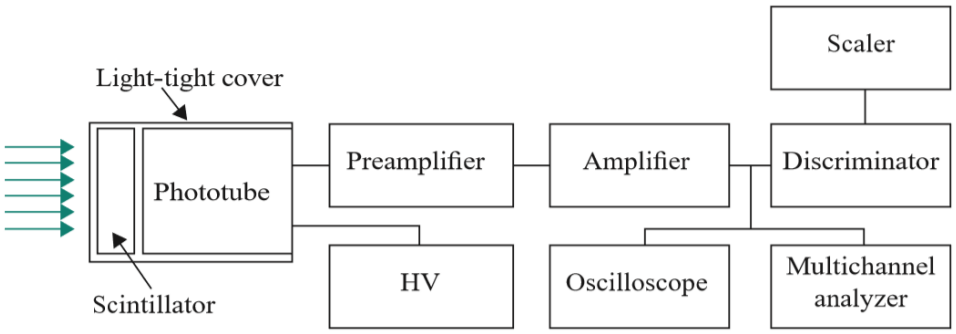

Figure 3.3: A detection system using a scintillator

3.3.1 High voltage power supply

A high voltage power supply (HVPS) is the power unit of a detector and provides a positive or negative voltage required for the detector operation. High voltage power supplies are

designed in such a way that for any fluctuation of input voltage causes very little change in the output voltage.[20]

3.3.2 Preamplifier

A preamplifier is an essential part of the radiation detection system that provides an optimized coupling between the output of the detector and the rest of the counting system. Preamplifiers play an important role to minimize sources of noise that may change the input signal.[20]

3.3.3 Amplifier

An amplifier in a detection system plays the important role of amplifying the signal and shaping it. This unit amplifies and converts the signal at the output of preamplifier into a suitable form for desired measurement. Commercial amplifiers can amplify the amplitude of input signals by as many as 2000 times in certain models. Regardless of the input signal and amplification, the maximum signal produced by any modern commercial amplifier has an amplitude of 10V. Amplifiers commonly have both coarse and fine gain controls for adjusting the amplification. Coarse gain adjusts the amplification in steps while fine gain does it continuously within each course gain step. Modern digital systems have built in amplifiers that are designed such that coarse and fine gains can be computer-controlled. Most commercial amplifiers produce bipolar or unipolar pulses at the output.[20]

3.3.4 Discriminator

The purpose of the discriminator is to reject unwanted signals. Every electronic system has some electronic noise. When a signal is amplified, electronic noise is also amplified with it which is unwanted. Unwanted pulses caused by electronic noise should not be counted. A discriminator or single channel analyzer eliminate this electronic noise. In some cases, particles above or below certain threshold energies or within some energy range are desired

to be counted by the detection system. The discriminator is the unit of the detection system that selects pulses corresponding to the desired particle energy.[20]

3.3.5 Scaler

The scaler is the pulse recording unit of the detection system. A scaler counts every pulse that enters into it and a count of one is added to the previous total number of counts. Thus it provides the total number of pulses recorded at the end of the counting period.[20]

3.3.6 MultiChannel analyzer

The multichannel analyzer or MCA is the instrument in the detector system that measures the energy spectrum of a radioactive source by recording a pulse height distribution of the pulses produced by the particles emitted from the source. MCAs can be used in two different modes: either Peak-height analysis (PHA) mode or Multichannel Scaling (MCS) mode. In PHA mode incoming pulses are sorted according to their heights and number of pulses of a particular height are stored in a corresponding particular channel of MCA memory. In MCS mode events are counted as a function of time. Each individual channel records the number of incoming pulses of all energies within a particular preset time interval. After that time period, pulse counting operation is automatically switched to the next channel.[20]

3.4 NIMbin

NIM is the abbreviated form of the "Nuclear Instruments Module" which is the oldest nuclear electronics standard developed by the US Atomic Energy Commission. Most of the commercially available instruments used in radiation measurement conform to the NIM standards. The purpose of the NIM standards is to permit the design of commercial modules that are physically and electronically interchangeable. The electrical interchangeability is confined to the power supply of the modules and generally independent of the internal circuit design.

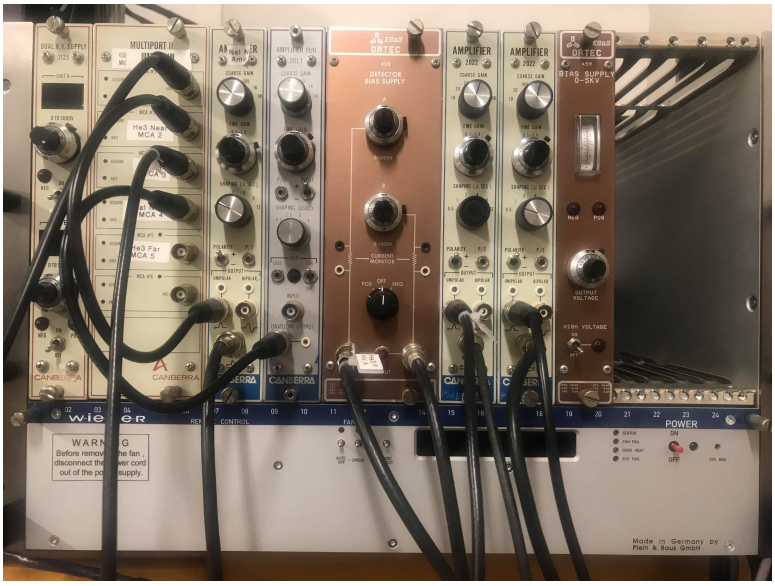

Figure 3.4: NIMbin

3.5 Genie-2000 Basic Spectroscopy Software

GENIE−2000 is a comprehensive environment for data acquisition, display and analysis of gamma and alpha spectrometry data from Canberra Industries, Inc. This media contains the basic spectroscopy functions for GENIE-2000. Functions provided with this software include: hardware acquisition and control, live spectral data display, energy/shape/efficiency calibration, peak analysis, and reporting. Genie2000 basic spectroscopy software provides independent support for multiple detectors, extensive networking capabilities, an intuitive and interactive human interface and comprehensive batch procedure capabilities. This software's multitasking architecture allows it to run multiple independent count procedures for several detectors simultaneously. No procedure is suspended by the activation of another or caused to slow down excessively by software overhead. With Genie 2000 software, operation is fully independent.

3.6 Lead collimator column

For the first experiment, a collimator structure with two rectangular apertures was built by placing a few lead bricks in an ordered manner. The height of the total collimator structure

was 22".Two rectangular apertures of the collimator structure were 9.5" apart and each had dimensions of 4.0" $\times$ 2.0" $\times$ 0.5". In the second experiment, a vertical lead collimator column

(a) Lead brick structure for the 1st experiment

(b) Lead block column for the 2nd experiment

Figure 3.5: Collimator

was built from four lead blocks. Each block has two rectangular slits to channel the emitted radiation towards the detector placed in front of it. The dimensions of each of the lead block was 4.0" $\times$ 4.0" $\times$ 2.0". The collimator was designed and built in such a way that all the slits in four lead blocks of the collimator were separated from each other by the same distance of 1.80".The dimensions of each collimator slit was 1.5" $\times$ 2.0" $\times$ 0.2". Before drilling the lead blocks to make collimator slits, a drawing of collimator slits and their dimensions considering the projection of the detector aperture was made to get a good assessment of collimator-detector system in the experimental set up.

3.7 Syringe pump

A syringe pump is a small infusion pump that can administer a small amount of fluid to a system gradually. In the present experiment, a KdScientific Legato100 series single-syringe pump was used to inject radioactive salt solution into the packed bed system. It is an infuse only syringe pump and capable of accommodating syringes from 0.5μl to 60ml. Infusion volume of the pump can be controlled by user definable flow rates with selected target volume or time values.

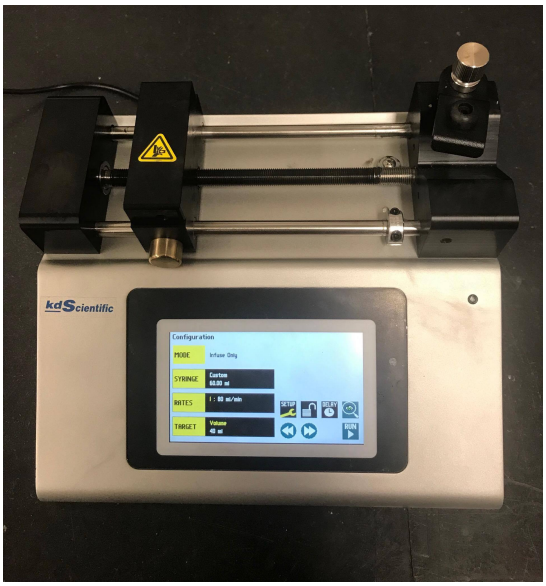

Figure 3.6: Syringe pump for injecting radioactive salt solution to the packed bed

3.8 Conductometer

To measure the conductivity of the salt solution for the experiment of the present research work, a Rosemount 1056 dual channel transmitter was used. It is a dual input analyzer which can display up to two independent liquid measurements. A Rosemount 1056 dual channel transmitter is a line powered device and capable of accepting inputs from PH/ORP, ISE, flow, conductivity (contacting and toroidal), turbidity and armperometric (dissolved, oxyzen, chlorine and ozone) sensors. Inputs are isolated from signal sources and earth ground

to ensure clean signal input. Standard 0/4-20mA current outputs can be programmed to correspond to any measurement or temperature.

Figure 3.7: Conductometer

3.9 Fume hood and chemical laboratory facilities

A fume hood or fume closet is a kind of local ventilation device designed to limit exposure to hazardous or toxic fumes, vapors or dust. For the Na-24 radiotracer experiment in this research work, NaCl solution was prepared from irradiated sodium carbonate sample. Under the fume hood facility, dissolved sodium carbonate solution was titrated with hydrochloric acid to prepare desired sodium chloride solution. Burette, pippette, conical flask and glass beakers were the laboratory tools required for the titration process.

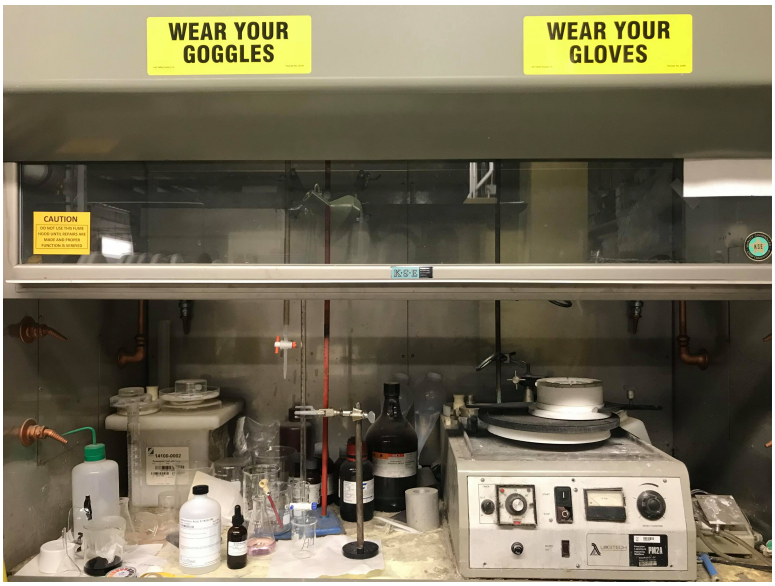

Figure 3.8: Fumehood and chemical laboratory facilities for titration

Chapter 4

Design of experiment & MCNP model simulation

4.1 Design of the Experiment

A radiotracer experiment involves many steps. The experiments described here involved a tracer strategy, selection of appropriate tracers, preparation of a safety report that was submitted to the relevant authorities, preparation of tracer mixture, calibration and quality assurance, selection and design of tracer injection and sampling procedures, transportation of tracer to the injection site, implementation of radiation safety procedures at the injection site, radioactivity contamination survey, injection equipment decontamination and radioactive waste handling, tracer sampling and sample transportation to analytical laboratory, tracer analysis, simulation of the deetector response, evaluation of data, and reporting of results[23].

In this present research work, two radiotracer experiments were designed that modeled the deposition of dissolved impurities in a debris bed upon injection of salt water. In both experiments, a packed bed was formed into which the radioactive salt water was injected using a syringe pump. Salt deposition was inferred by analyzing the responses of the detectors as a function of time. For each experiment, a detector system was devised for the detection of radiation released from radioactive salt. Lead collimator structures were built

and placed in between the packed-bed and the detectors to collimate the radiation from the bed toward the detectors. The constituent particles used for the formation of the packed bed were mostly alumina particles, color changing-cation exchange resin and, in the second experimeny, borosilicate particles. The purpose of using resin was to exchange the cations with salt particles which would lead to the measurement of salt deposition in the packed bed. The resin color change would help to monitor the salt adsorption with time in different locations of the packed-bed resin during the salt water flow. The radioactive salt water was injected from the top of the packed-bed and after the flow through the bed residuals were collected in a beaker placed underneath the glass tube.

In the first experiment a 12" glass tube contained the total packed bed. NaCl salt solution containing Na-24 radio tracer was pumped into the packed bed. Na-24 is a short-lived radioisotope with a half life of 14.9 hours. It spontaneously emits gammas of 1,365 KeV and 2,754 KeV. Two NaI detectors were placed near the top and bottom ends of the tube for the measurement of gamma radiation emitted from radioactive NaCl flowing or deposited in two respective locations. The detector system and the packed bed was separated by a lead brick collimator structure.

The second experiment was designed to study the salt deposition in four different locations of a packed bed using a system of four NaI detectors. A similar kind of packed bed as the fist experiment with a larger size of 16" packed bed height was formed. An improved collimator structure formed with four lead blocks each having two collimator slits of 0.2" aperture height respectively was placed in between packed-bed and detector system. In the second experiment Sr-84 was used as radiotracer and radioactive $SrCl_2$ salt solution was injected into the bed to estimate the spatial distribution of salt deposition within it.

4.2 Radiotracer Selection

The selection of a suitable radiotracer is of prime importance for a radiotracer experiment. The tracer should represent the stream it is tracing. Often, it is possible to select a representative tracer on the basis of experience, from published references or from a physical and

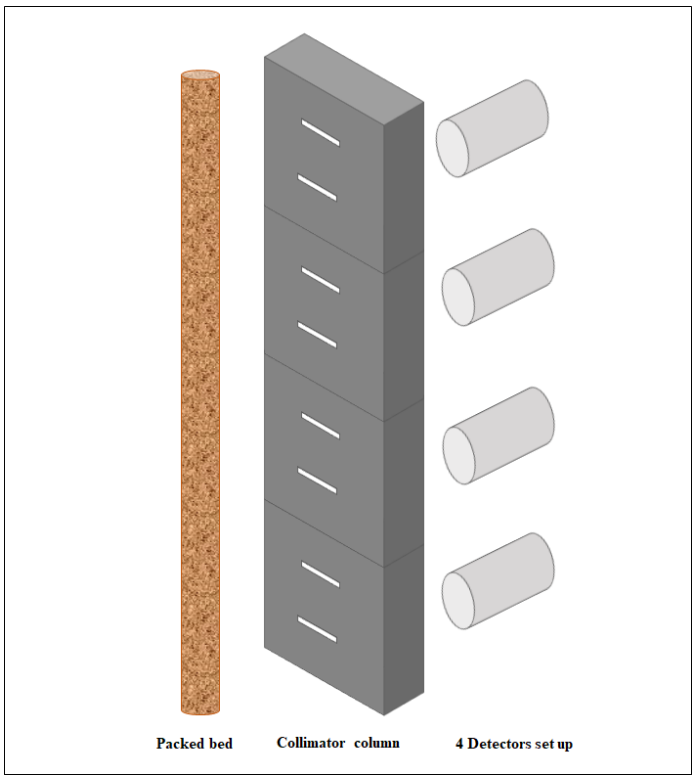

Figure 4.1: Design of Sr-85 radiotracer experiment.

chemical evaluation of its compatibility with the stream to be traced. If necessary, however, the suitability of the tracer must be confirmed by validation tests in the laboratory[24]. Factors that affect radioisotope selection are (1) availability (2) cost (3) half-life, and (4) energy of emitted radiation[21]. In the present research work, two radiotracer isotopes, Na-24 and Sr-85, were selected considering all the above factors of radioisotope selection along with the essential fact that NaCl is one of the main components of sea water and $SrCl_2$ acts as a surrogate of another sea water component $CaSO_4$ of similar solubility.

4.3 Na-24 Radiotracer Experiment

4.3.1 Experimental set up

A homogeneous mixture of alumina and resin particles was randomly packed in a glass tube. The top fitting of the tube was connected to a syringe pump via a Tygon® fitting to inject

NaCl salt solution tagged with Na-24 into the packed bed. Two 3×3 NaI scintillator detectors were used to measure the radiation emitted from Na-24 decays. A collimator structure was built using lead bricks and lead sheet and produced two rectangular apertures that allowed radiation to reach detectors (as shown in Fig.4.2). Each aperture was approximately 2.5cm wide and 0.5cm high. The distance between the detector and collimator aperture was approximately 1.27 cm and the elevations of the two detectors were approximately 25.4 and 50.8 cm above the local ground. The two detectors were calibrated with two check sources, Cs-137 and Co-60.

Figure 4.2: Detector-collimator set up for Na-24 radiotracer experiment

4.3.2 MCNP simulation for design verification

An MCNP model was developed to assess the total activity needed in the salt solution to generate sufficient response in the detectors within 10 second intervals to be able to estimate concentration of deposited salt in the bed. The experimental design criterion was selected on the basis of uncertainty in the estimated concentration to be below 5%. In the simulated experiments, the total Na-24 activity was considered to be homogeneously distributed with alumina particles in a cylindrical system. The system then behaved as a homogeneous volumetric source that was collimated and projected towards a NaI detector. In the MCNP

simulation set up, the geometry of the source-detector-collimator system was similar to the experimental set up. A total of 10^7 histories were simulated to estimate detector counts for 1.365-MeV gammas emitted from Na-24 using the F8 tally in MCNP. The MCNP output resulted in 1.518×10^{-4} (Note: Ruhania, give the standard deviation also) counts under the 1.365-MeV gamma peak per particle simulated. Based on these results it was estimated that approximately 100 - 200 μCi of Na-24 activity was sufficient for the experimental plan. This MCNP model was also used to interpret the experimental radiation counting data and estimate the concentration in the bed at different times during the experiment.

4.3.3 Na-24 radiotracer isotope preparation

For the experiment, Na-24 tracer isotope was prepared by irradiating a sodium carbonate sample in the IRIS port of the Kansas State University TRIGA reactor. A $5mg$ sodium carbonate sample was taken in a small plastic vile and irradiated at $400KW$ reactor power. After irradiation, the sodium carbonate sample was left to decay for one hour. The beta and gamma exposure rate at one foot from the sample was recorded to be $35mR/h$ after the one hour waiting time, which was considered to be sufficiently safe for handling. The irradiated sodium carbonate sample was dissolved in $100ml$ deionized water to make a $0.006M$ sodium carbonate solution and a few drops of phenolphthalein were added to it. Finally a sodium chloride solution was prepared by titrating the sodium carbonate solution with $0.1M$ hydrochloric acid.

4.3.4 Experimental procedure

The packed bed glass tube was placed in front of the collimator assembly in such a way that both the top and bottom ends of the packed bed were facing the two detectors through the collimator apertures. High voltage power supplies, multichannel analyzers, amplifiers and other required electronics for both detectors were put in place. Sodium chloride solution was prepared from the chemical reaction of irradiated sodium carbonate and hydrochloric acid. The chemical process of making sodium chloride was performed carefully following

appropriate radiation safety procedures. Two percent by weight sea salt (NaCl) was added to the radioactive solution to increase the adsorption rate in the ion exchange resins resulting in local saturation. The conductivity of the solution was measured with a conductometer. A 60 ml sample of the final solution was then taken to the syringe and pumped to the packed bed at 10 ml/min flow rate for 5 minutes. Counting data were collected for both detectors in 10-second time steps followed by 10-second delay to save the data, over a total period of 5 minutes. The residual solution draining from the packed bed outlet was collected in a beaker over the total period of the experiment.

4.4 Sr-85 Radiotracer Experiment

4.4.1 MCNP model development and simulation

The MCNP model developed for Na-24 radiotracer experiment was upgraded with Sr-85 source and new geometry for the collimator column in the Sr-84 radiotracer experiment. In the new MCNP model, a source concentration was incorporated by source biasing. The distance between source and detector-collimator system was similar to the experimental set up. The MCNP model had small volumetric source with a height of one inch. Dimension of the MCNP model source was approximately identical with the portion of the packed bed exposed toward a detector. In MCNP only the a single slit lead collimator block and one NaI detector were modeled as each pair of slits in all four collimator blocks in the experimental set up were identical in dimensions. Therefore the simulation result of the model with one collimator slit and one detector would be applicable for all four detector with double slits. The model was simulated for estimating detector response like the previous MCNP model applying the F8 tally in MCNP input. Sr-85 emits gammas of 514 keV. So in the MCNP model 10^7 particles were simulated to estimate the NaI detector response for 514 keV gammas.

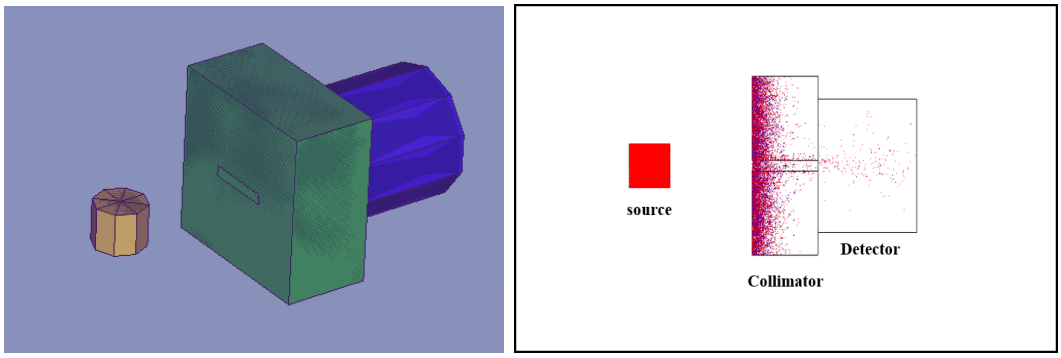

(a) 3D plot in vised for MCNP model of source-detector-collimator system

(b) 2D plot of particles track in Vised for the MCNP model simulation

Figure 4.3: Geometry of the MCNP model for the Sr-85 radiotracer experiment.

4.4.2 Detector and collimator set Up

A vertical column of lead collimator blocks was set up. Four NaI detectors were placed in front of the collimator structure such that each detector aperture faces two collimator slits of a lead block. Detectors were connected to the associated electronics (power supply, amplifier, Multiport II) in a NIMBIN, which was connected to a computer. All the detectors were shielded properly with thick lead sheets from two sides and top.Gamma acquisition and spectroscopy software was turned on and data sources(each of the four detectors had its won MCA) were opened in the software. All MCAs were set up for radiation counting. Background radiation counting was recorded for all four detectors simultaneously in Multi-channel scaling (MCS) mode. After saving the recorded counting data files, data sources (MCAs) were cleared and set up for next radiation counting of the four detectors.

4.4.3 Formation of the packed bed

To form a packed bed, a cylindrical glass tube was taken and rinsed well with deionized water. The tube was dried and a small round shaped filter was placed at the bottom end of the glass tube. A 1:3 mixture of borosilicate particles and alumina particles was inserted into the tube. A nuclear grade mixed bed color changing DI resin was added to the alumina-borosilicate mixture of the packed bed. The glass tube was shaken well so that resin particles could spread in between the other types of particles. It was intended that the mixture of resin,

Figure 4.4: Collimator-detector set up for Sr-85 radiotracer experiment

alumina and borosilicate particles would be homogeneous. Fitting and tubing were connected to the packed bed glass tube. At last, the packed-bed tube was mounted with caution in front of the detector-collimator set up in such a way that eight different locations of the bed from top to bottom were exposed to the four detectors through collimator slits. A beaker was placed below the mounted packed-bed tube to collect the residue of the radioactive salt solution infused to the bed.

4.4.4 Preparation of radioactive salt solution

A salt solution was prepared by adding 3.5g NaCl in 100ml deionized water. A 25 micro litre salt solution was taken out using a pipette and introduced into the small vial containing radioactive Sr-85 solution. The source vial contained 27.8 micro litre Sr-85 solution with an activity of 500 micro curie. Next 50 micro litre solution was taken out from the source vial using the pipette and added to 60ml salt solution contained in a separate beaker. The solution was stirred well to mix the radioactive Sr-85 solution to the NaCl salt solution

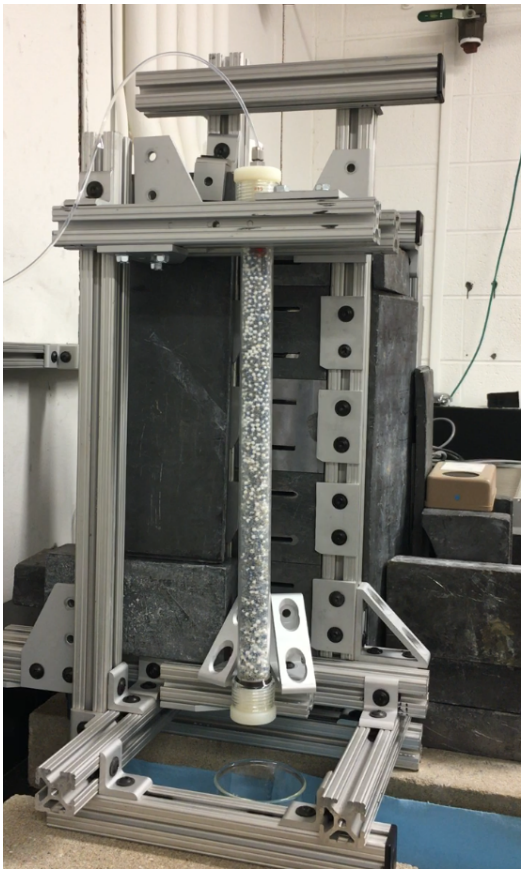

Figure 4.5: Packed bed

properly.

4.4.5 Measurement of conductivity

After preparing the radioactive salt solution,its conductivity was measured using a conductometer. Before the measurement, two probes of the conductometer were rinsed with deionized water and dried off. Later two probes were connected to the conductometer. One probe was immersed into the radioactive salt solution. and the conductivity measured by the meter was recorded.

4.4.6 Conduct of the experiment

To begin, 50ml of the radioactive salt solution was taken into a syringe. The syringe was placed on the syringe pump with extra caution to avoid any spill of radioactive salt solution.

Figure 4.6: Conductivity measurement of salt solution

Coupling between syringe and the packed bed was established by connecting required fittings and tubing. The syringe pump was turned on and the target volume was set to 50ml with a 10ml/min infusion rate. When ready, the syringe pump and detectors were started. The starting time of the experiment run was noted and different times for resin color change near each detector slits were recorded with a stop watch. Solution passed through the packed bed was collected in a beaker placed under the packed bed tube. It took 5 min for the syringe pump to infuse 50 ml radioactive salt solution into the packed bed. The multiple detection system kept collecting radiation counting data for a period of 1024 seconds. The end time of the experiment was recorded as soon as the detectors stopped counting radiation. At the end of the experiment the conductivity of the residual solution was measured again.

4.4.7 Disposal of radioactive waste

At the end of the experiment, the packed bed along with syringe and tubing were carefully removed from the mounting structure. While removing the packed bed with caution, a

beaker was held below the packed bed tube in order to collect any radioactive solution that might spill. All the packed bed particles were removed from the tube and stores in a plastic bottle. The radioactive salt solution was separately stored in a plastic jar. All other contaminated items along with the plastic jar and the bottle containing radioactive particles and salt solution were disposed in a waste box. The waste box was taped and radiation safety stickers were attached to it according to the radiation safety and handling guide book. A tag with all required information (radioisotope, radiation dose rate, list of contaminated stuffs) was attached to the waste box. Finally the waste box containing radioactive waste was handed over to the radiation department staff.

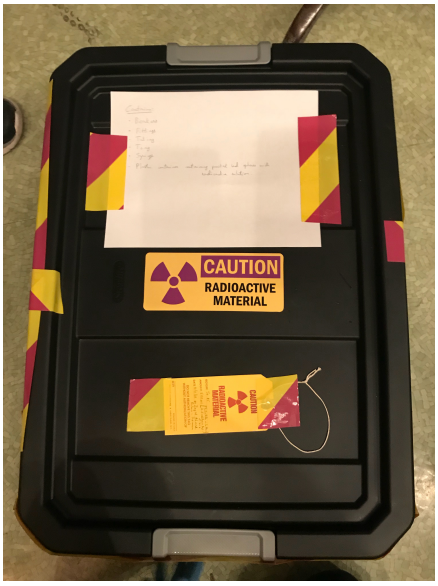

Figure 4.7: Box containing radioactive waste and contaminated items.

Chapter 5

Results & Discussion

5.1 Result analysis of Na-24 radiotracer experiment

In the Na-24 radiotracer experiment, NaCl salt solution containing Na-24 radiotracer was injected into the packed bed at constant flow rate to study the salt deposition in the packed bed. Apart from the radiotracer, there were two alternative ways to monitor the salt mass transfer from solution to the packed beds. Before injecting into the packed bed, the conductivity of salt solution was measured to be $28mS/cm$. But the conductivity of the collected salt solution in the beaker after passing through the packed bed was measured to be less than $10\mu S/cm$, which is comparable to de-ionized water. The lower conductivity of the solution that was collected after flowing through the bed provided an indication that there were few or no ions left in the solution. Therefore, it was obvious that salt particles in solution were mostly adsorbed in the packed bed.

While the radioactive salt solution was percolating through the packed bed, the color of the resin from the upper section of the packed bed started to change, which served as another method to monitor the presence of salts in the bed. The packed bed resin color was bluish at the beginning of the experiment. As soon as the salt solution was injected into the packed bed, the resin started changing its color as it adsorbed dissolved solids from the salt solution. It can be concluded from the blue-colored resin of the lower part of the packed bed

that ions in the salt solutions were completely adsorbed by the resin from the top half of the packed bed.

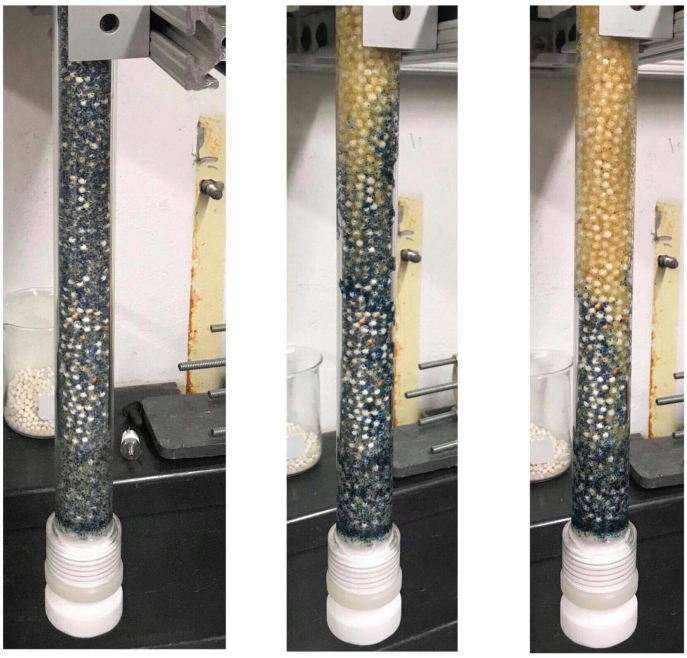

Figure 5.1: Resin color change in packed bed due to adsorption of NaCl salt particles in the resin.

These alternative methods were able to provide a qualitative understanding of the change in salt adsorption or de-ionization of the solution, but they were insufficient for quantitative estimates. The radioactive tracer method is used for quantitative estimation of salt deposition rate and local mass transfer. From the detector counting data, it was observed that the counts for the top detector increased with time until it became approximately constant for several time steps. On the other hand, the detector located near the bottom end did not show any significant increase in net counts throughout the experiment. During the first time steps, salt solution was just injected into the system therefore no significant adsorption or no net Na-24 emissions were detected. After two time snapshots enough radioactive salt solution had entered into the packed bed which caused the dissolved ions including Na-24 to adsorb on the resins and the top detector started counting gamma rays emitted by radioactive Na-24. The increase in counts was observed due to increased amount of salt adsorbed in the top section of the packed bed. After a few time steps the counts for the top detector

became approximately constant as due to high salt concentration i.e. 2.0% or $\sim 2.0 gm/ml$. Meanwhile total counting data profile did not show any variation for the bottom detector as radioactive sodium of the solution was mostly adsorbed by the resins from the upper section of the packed bed. Almost no radioactive sodium reached the bottom part of the packed bed which is consistent with the visual observations of no color change in the resins at lower end of the bed.

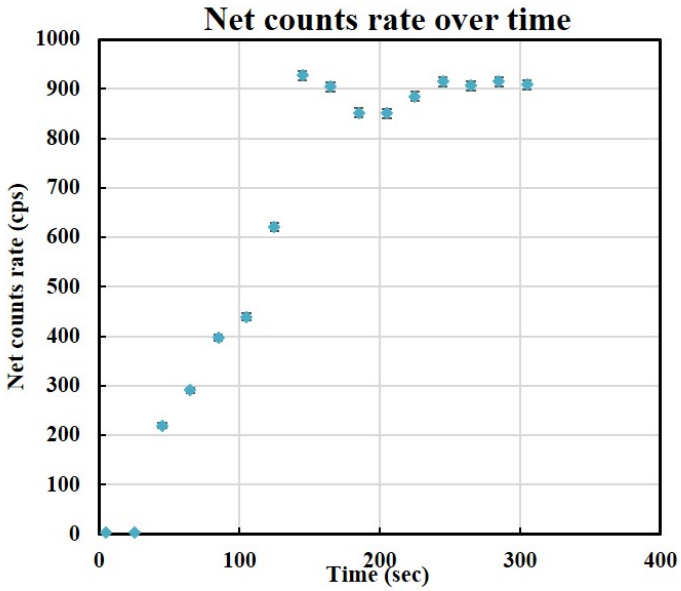

Figure 5.2: Net counts rate Vs time plot for the top detector

The activity of Na-24 over time can be determined by the equation 5.1 using the MCNP simulation results for counts/particle and the experimental net count rate. Activity of any radioactive sample is proportional to the number of counts detected and related to the detector response as:

$$\frac{A_t(t)}{R_t(t)} = \frac{A_m}{R_m} \tag{5.1}$$

where, A is the local activity in the test region (region of the packed bed exposed towards the collimator and detector), R is the detector response. The subscripts t and m represent experimental domain and MCNP model, respectively. Mass of radioactive salt deposits has

a proportional relationship with the activity of the salt. So locally deposited mass also possessed a proportional relation with the detector response as follows:

$$\frac{M_t}{R_t} = \frac{M_m}{R_m} \tag{5.2}$$

where, M_m is the mass of radioactive salt uniformly deposited through the test section. M_t is the mass of local salt deposits in experimental domain. R_m and R_t represents the detector responses due to the uniform activity in test section of MCNP domain and local activity in test section of the experimental domain, respectively. In the Na-24 radiotracer experiment, the amount of activity present in the packed bed system due to radioactive NaCl salt was $170\mu Ci$. The activity $170\mu Ci$ is equal to $62,90,000Bq$ or disintegrations/sec. The amount of radioactive Na-24 mass corresponding to this activity is $1.94 \times 10^{-11}g$. In Na-24 radiotracer experiment the height of each collimator aperture was 0.5 inches and the height of the packed bed was 18 inches. So it could be considered that the packed bed was a combination of 36 sections each having a height of 0.5 inches and two sections were directly exposed to two detectors through the collimator apertures. In the MCNp model of the Na-24 radiotracer experiment, the total activity within the source packed bed was considered uniformly distributed. The simulation results of the MCNP model provided $0.00015 \pm 0.000003855 counts/particle$ detector response for each particle simulation. So it is estimated from the MCNP that the detector response would be $26.52 counts/sec$ if $6290000Bq$ is uniformly distributed in the packed bed. The local radioactive salt mass deposition in experimental domain was estimated calibrating the MCNP simulation results with the experimental radiation count rate using the above equation 5.2.

The detector response signal in the form of total counts over a period of 10 seconds was used to estimate count rate and then mass of salt deposits evolving over the duration of experiment. The net count rate profile for the detector response over time (fig.5.2) shows that the net count rate of the top detector initially increased with time but became constant after sometime of the experiment. The net count rate started to increase as soon as radioactive salt was injected into the packed bed and approached an approximate average value of

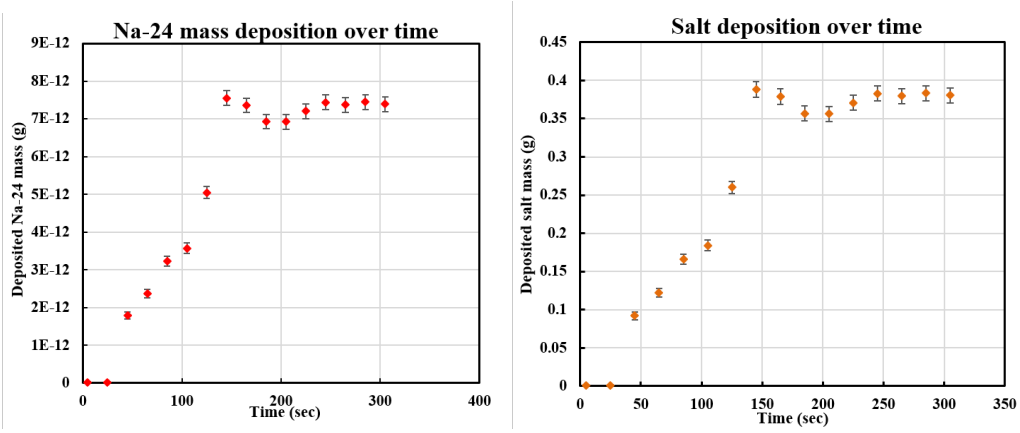

(a) Na-24 mass deposition Vs time plot (b) Salt mass deposition Vs time plot

Figure 5.3: Mass deposition over time plot.

910.875$counts/sec$ as the salt deposits saturated in packed bed resin at the location near the top detector. The deposited salt mass vs time plot (fig. 5.3) also shows the similar profile. The deposited salt mass in the test region near the inlet increased during the initial time steps. After few time steps of the experiment the salt deposits reached saturation in packed bed resin. The mass of the Na-24 deposits was estimated $7.41 \pm 0.21pg$ scaling the MCNP simulation results of detector count rate with experimental count rate considering 40% void fraction in the packed bed.

5.2 Result analysis of Sr-85 radiotracer experiment

5.2.1 Salt deposition and color change of packed bed resin

In this present salt deposition study, resin was employed in the experiment design as a part of packed bed component to allow the salt in solution deposited in the system. The salt deposition pattern thoroughly depends on the amount of resin and its distribution into the packed bed. In the second radiotracer experiment, a packed bed was formed with alumina, borosilicate particles and resin and Sr-85 salt solution was injected into the bed. Immediately after the infusion of radioactive salt solution into the packed bed, the resin of the bed started to change its color which was similar as the result of the Na-24 radioactive tracer experiment.

The resin color turned yellow from its original blue color which suggested that the salt in the solution had been deposited in the packed bed by exchanging its cations with resin. Figure shows that the resin color changed over time from the top to the bottom of the packed bed as the salt solution flew through the system. The observed pattern of the resin color change unfolds the trajectory of the solution flow and the spatial distribution of salt deposits within the packed bed.

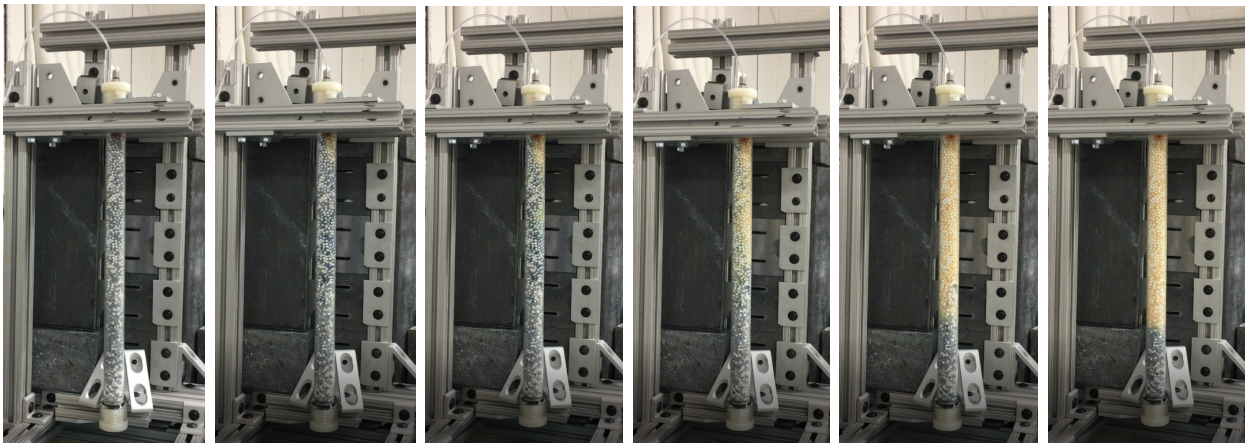

Figure 5.4: Resin color change in packed bed due to salt deposition

5.2.2 Analysis of multiple detector response data

In the second experiment with salt solution containing radiotracer Sr-85, a multiple detector system of four NaI(Tl) detectors recorded the gammas emitted from four respective locations in the packed bed where salt particles locally deposited. Before injecting radioactive salt solution into the bed, Background radiation data was recorded by the four detectors co-currently for a period of 1024 seconds. The fig 5.5 shows the background radiation recorded by detectors-1, detector-2, detector-3 and detector-4 were approximately 20 cps, 20 cps, 19 cps and 26 cps respectively.

During the experiment, syringe pump and the multiple detectors were run simultaneously to detect the gammas emitted from radioactive salt solution while flowing through the packed bed. The radiation counting data was recorded by the four detectors for the same period of background counts. The figure shows the four detectors net responses over the same period of

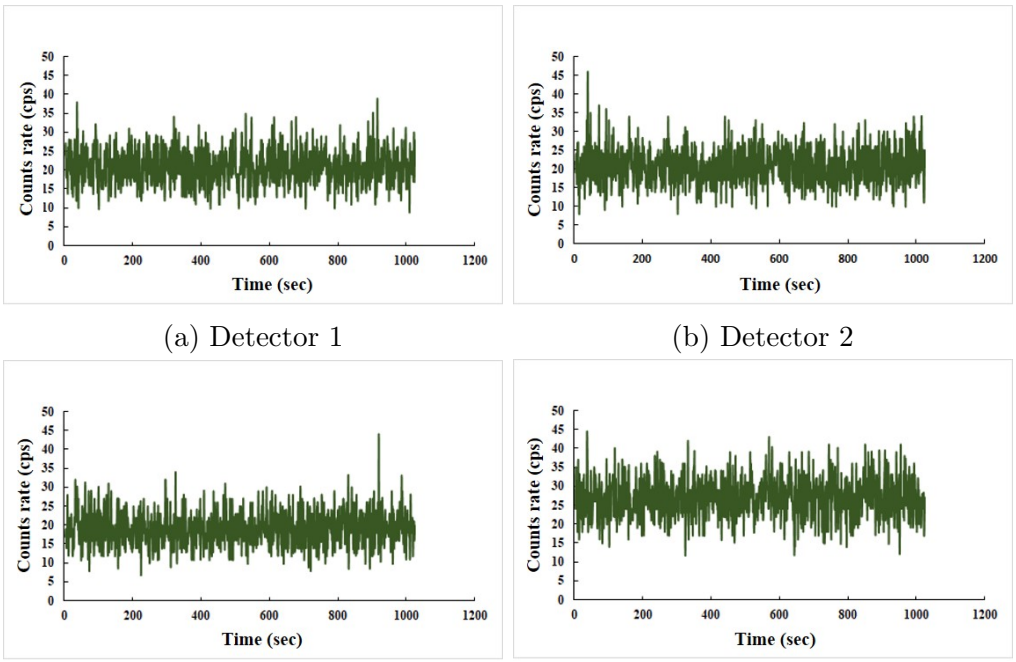

(a) Detector 1

(b) Detector 2

(c) Detector 3

(d) Detector 4

Figure 5.5: Background counts rate for four NaI(Tl) detectors

time. It is visible from the net counts plots for four detectors that net counts increased with time except for detector 3. Detector-1 response shows that the net count rate increased until it reached a saturation where the net counts was around 599 cps on an average. Similarly detector 2 and 4 net counts increased with time and saturated approximately around 107 cps and 54 cps respectively. Apparently the pattern of the net counts profile was similar for detector-1, detector-2 and detector-4. It is observed from the net counts plots for three detectors(1, 2 and 4) that initially the detected net counts for all three detectors were very low(near background). The detector response profile showed that the counts increased faster for detector-1 and it kept increasing while the other two detectors net counts increased very slowly compared to detector-1. It is evident from the net counts plots that all three detectors (1, 2 and 4) reached to their saturation phase near the same time which is approximately after 300 seconds from the initiation of detector counting . This pattern of increasing net counts and saturation at different net count values for different counters can be explained with the radioactive salt deposition in packed bed over time.

At the beginning of the simultaneous run of the radioactive salt infusion and detector

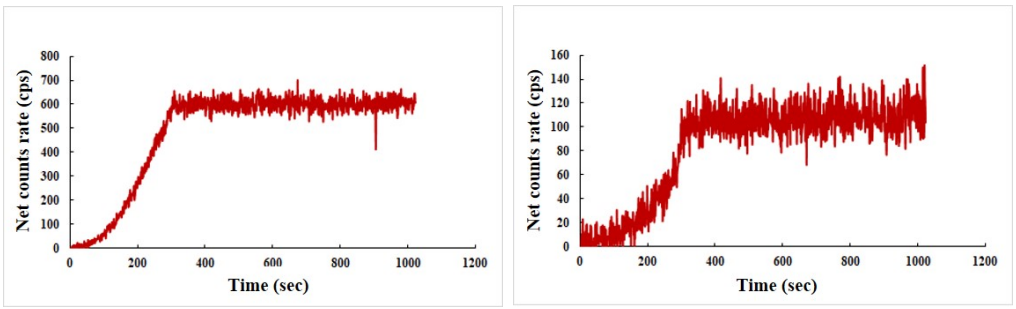

(a) Net counts for detector 1 (b) Net counts for detector 2

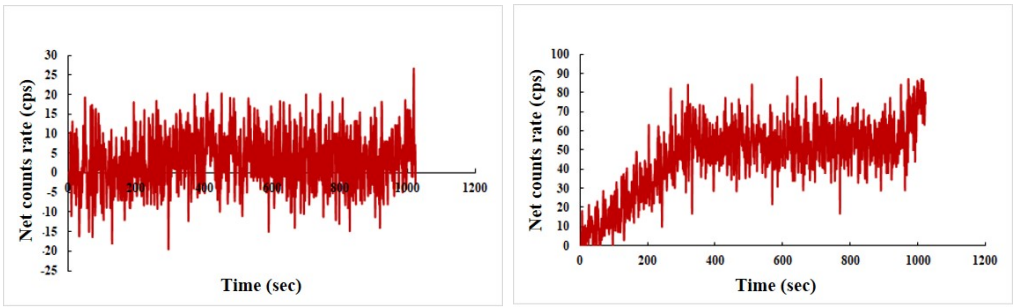

(c) Net counts for detector 3 (d) Net counts for detector 4

Figure 5.6: Detector responses for multiple detector system

counting, no radioactive solution was present in the packed bed at the vicinity of the multiple detector system as it required few seconds for the salt solution to flow into the packed bed from the syringe pump through the connecting tube. As soon as the radioactive salt solution infiltrated the packed bed, salt particles started to deposit in resins of the bed. Radioactive salt solution and salt deposits were first observed by the detector 1 as it is placed near the top of the packed bed. Radioactive salt particles were adsorbed in resin layers while solution flew through the bed. So the concentration of the salt solution varied during the flow. When the solution in the bed reached at the proximity of detector-2, it contained reduced concentration of salt and less radioactive salt deposited in the resin of the bed. This explains the less net counts at saturation for detector-2 compared to detector-1. Similarly when the solution finally approached the bottom part of the packed bed and close to the projection of detector-4, the salt concentration became very low so that very less amount of salt particles left in the solution to get deposited in the resin. This indicates why detector-4 had the lowest measured net count rate at saturation among all three detectors (1, 2 and 4).

The net counting data profile for detector-3 completely deviates from the pattern showed

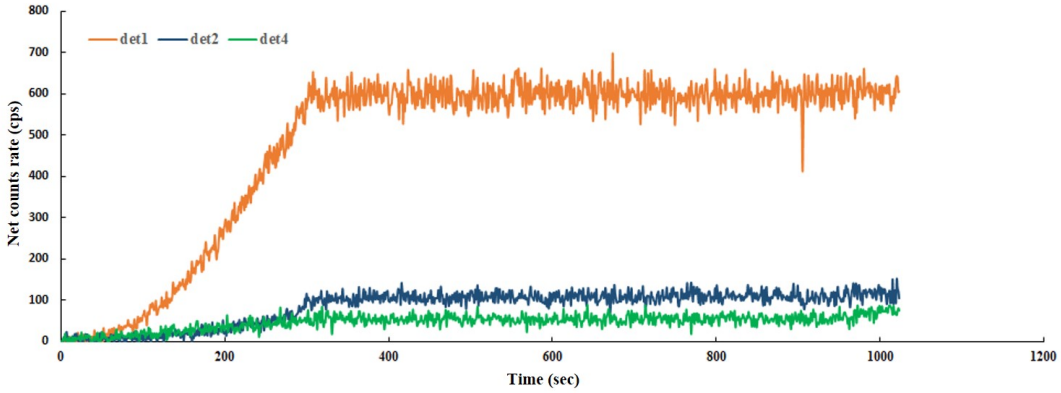

Figure 5.7: Comparison for three detectors net responses

by the other three detectors. A similar net counts vs time plot was expected for detector-3 response. A slow increasing detector response over time with lower saturation net counts compared to detector-1 and detector-2 but faster increasing gamma response profile with higher saturation net counts than detector 4 was desired for detector-3. But detector-3 response was utterly different from the rest of three and only comparable to the detectors background counts profile.

The counting data profile collected by the detector-3 can be explained in terms of the packed bed formation. The packed bed under study for salt deposition distribution couldn't be considered to be formed with complete homogeneous mixture of alumina, resin and borosillicate particles. The mixture had inhomogeneity and it is possible to have regions in the packed bed where no resin or very small amount of resin was present to exchange cations with salt compound of the solution. So it can be inferred that as there wasn't enough resin to adsorb salt, deposition was less or absent in the region near the detector three so that its gamma radiation counting data due to radioactive salt deposits was insignificant. That's why detector-3 recorded only radiation counts slightly above the normal background, as shown in fig 5.8

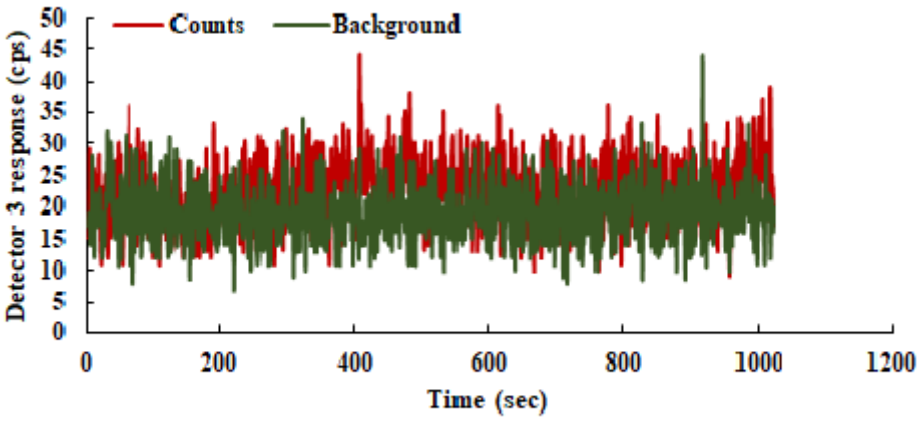

Figure 5.8: Detector-3 responses for radiation counts and background.

5.3 Calculation of local activity and radioactive salt mass deposition

Salt particles were deposited in the packed bed. The mass of salt deposits in a particular location can be measured from the activity accumulated there locally. Activity of the salt is proportional to the detector response. The detector response MCNP model simulation resulted for detector-1 is 433 counts/sec. So from the relation 5.1 the activity of radioactive salt deposits is determined $27.21 \pm 1.11 \mu Ci$. Similarly the individual detector responses for detector-2 and detector-4 were 446 counts/sec and 449 counts/sec provided by the MCNP model simulation under the corresponding LLD condition of two detectors. Correlating the MCNP results with experimental counting data of detector-2 and detector-4 respectively, the determined activity accumulated within the packed bed were $4.72 \pm 0.45 \mu Ci$ and $2.36 \pm 0.32 \mu Ci$. This result is expected as radioactive salt mostly adsorbed by resin in the upper layers of the packed bed. So higher accumulated activity was determined for detector-1 radiation counts. Salt solution that flew to the lower layers of the bed had lower concentration of radioactive salt so that less activity were determined for corresponding detector-2 and detector-4 counting data. The mass of radioactive salt deposits was calculated from the

local activity measurements using the following relation of activity and radioactive mass.

$$A = N\lambda \tag{5.3}$$

Here A is activity, N is the total number of particles and λ is the half life of the radioisotope. Using this relationship the mass of salt deposits corresponding to accumulated activities within the packed bed near three detectors were estimated $458.032 \pm 18.68pg$, $79.54 \pm 7.68pg$ and $39.82 \pm 5.4pg$ respectively .

5.4 Estimation of the packed bed locations for measured salt deposits

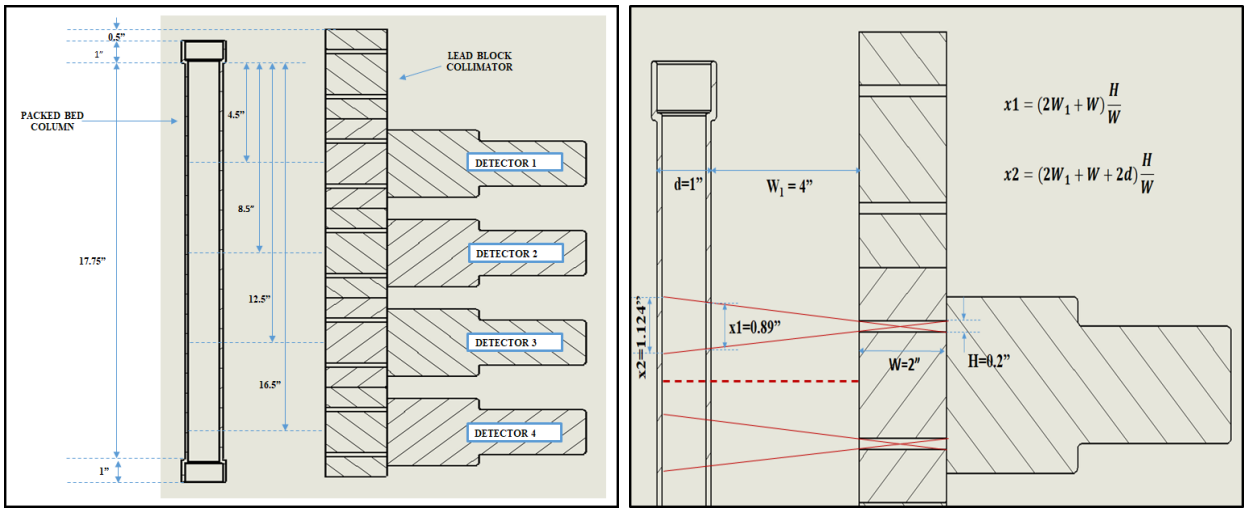

Figure 5.9: Sketch for estimating area for local salt deposition

During the salt solution flow through the packed bed salt particles were deposited in different locations of the packed bed. Detectors recorded the gamma counts released from radioactive salt particles. The local activity and the corresponding mass of salt deposits was estimated from the correlation of MCNP output and experimental counting data of four detectors. The locations of measured salt deposits can not be determined certainly but an approximate estimation of the salt deposition area is possible by solid angle calculation for

four detectors. The solid angle calculation provides the estimate of the region exposed to the each collimator aperture of a detector in multiple detector system. From the solid angle calculation it was found that approximately $0.89 inches$ to $1.12 inches$ height of the packed bed was exposed to each collimator slit. So the volume within approximately $2.0 inches$ height of packed bed in front of each detector could hold the salt deposits, radiation from which emitted towards the detector through collimator aperture.

5.5 Conclusions

Two radiotracers were used to investigate mass transfer and deposition of dissolved salt particles in different locations of the packed bed systems. The data obtained from the radiotracer experiments were used as a basis for the assessment of actual level of radioactive salt deposition in the system. In this research work two radiotracer based experiments measured the mass of local salt deposits in a packed bed . In Na-24 radiotracer experiment, two axial locations of the packed bed were monitored by two respective NaI(Tl) detectors to determine the local adsorption of dissolved salt from the aqueous flow. Salt deposited in the packed bed resin by exchanging mutual cations and a qualitative analysis of salt deposition was performed by studying the resin color change over time during salt adsorption. In Na-24 radiotracer experiment, the top detector response became approximately an average value of $910.875 counts/sec$ when the radioactive salt deposition in packed bed resin reached at saturation. The mass of saturated Na-24 deposits was estimated $7.41 \pm 0.21 pg$ by analyzing the detector count rate. No significant detector response was observed in the bottom detector as most of the dissolved salt was adsorbed by the resin in the top half of the packed bed. In the second experiment, local activities of Sr-85, $27.21 \pm 1.11 \mu Ci$, $4.72 \pm 0.45 \mu Ci$ and $2.36 \pm 0.32 \mu C$ were estimated in three different axial locations of the packed bed. Mass of the radioactive salt deposits corresponding to three local activities were measured $458.032 \pm 18.68 pg$, $79.54 \pm 7.68 pg$ and $39.82 \pm 5.4 pg$ in packed bed locations near three respective detectors assumed minimal salt adsorption at the site near the other detector. In both experiments, deposited local activity and radioactive salt mass were determined by analyzing and calibrating the

detector responses in experimental domain with detector count rates for a simulated MCNP model that emulates the actual experiment.

Bibliography

[1] Menachem Elimelech, John Gregory, and Xiadong Jia. *Particle deposition and aggregation: measurement, modelling and simulation*. Butterworth-Heinemann, 2013.

[2] Keiko Tagami, Shigeo Uchida, Yukio Uchihori, Nobuyoshi Ishii, Hisashi Kitamura, and Yoshiyuki Shirakawa. Specific activity and activity ratios of radionuclides in soil collected about 20 km from the fukushima daiichi nuclear power plant: Radionuclide release to the south and southwest. *Science of the Total Environment*, 409(22):4885–4888, 2011.

[3] Fukushima Daiichi. Ans committee report. *A Report by The American Nuclear Society Special Committee on Fukushima*, 2012.

[4] Ken Buesseler, Michio Aoyama, and Masao Fukasawa. Impacts of the fukushima nuclear power plants on marine radioactivity. *Environmental science & technology*, 45(23):9931–9935, 2011.

[5] Ken O Buesseler. Fukushima and ocean radioactivity. *Oceanography*, 27(1):92–105, 2014.

[6] Yu Morino, Toshimasa Ohara, and Masato Nishizawa. Atmospheric behavior, deposition, and budget of radioactive materials from the fukushima daiichi nuclear power plant in march 2011. *Geophysical research letters*, 38(7), 2011.

[7] Tomoko Ohta, Yasunori Mahara, Takumi Kubota, Satoshi Fukutani, Keiko Fujiwara, Koichi Takamiya, Hisao Yoshinaga, Hiroyuki Mizuochi, and Toshifumi Igarashi. Prediction of groundwater contamination with 137cs and 131i from the fukushima nuclear accident in the kanto district. *Journal of environmental radioactivity*, 111:38–41, 2012.

[8] H Pant, A Saroha, and K Nigam. Measurement of liquid holdup and axial dispersion in trickle bed reactors using radiotracer technique. *Nukleonika*, 45(4):235–241, 2000.

[9] Rajesh Kumar, HJ Pant, VK Sharma, Sadhana Mohan, and SM Mahajani. Investigation of hydrodynamic behaviour of a pilot-scale trickle bed reactor packed with hydrophobic and hydrophilic packings using radiotracer technique. *Journal of Radioanalytical and Nuclear Chemistry*, 294(1):71–75, 2012.

[10] Mark Basset, Jeff Mcinerney, Norm Arbeau, and Derek H Lister. The fouling of alloy-800 heat exchange surfaces by magnetite particles. *The Canadian Journal of Chemical Engineering*, 78(1):40–52, 2000.

[11] G Horányi. *Radiotracer studies of interfaces*, volume 3. Elsevier, 2004.

[12] HJ Pant, Arunabha Kundu, and KDP Nigam. Radiotracer applications in chemical process industry. *Reviews in chemical engineering*, 17(3):165–252, 2001.

[13] Antonio R Ubiera and Giorgio Carta. Radiotracer measurements of protein mass transfer: Kinetics in ion exchange media. *Biotechnology Journal: Healthcare Nutrition Technology*, 1(6):665–674, 2006.

[14] H. J. Pant, Sunil Goswami, V. K. Sharma, S. K. Maity, and M. O. Garg. Flow investigation in an industrial-scale soaker using radiotracer technique. *Applied Radiation and Isotopes*, 124:119–123, 2017. https://doi.org/10.1016/j.apradiso.2017.03.012.

[15] Ki-Chul Kim, Geon-Hyeong Park, Sung-Hee Jung, Jung-Lyul Lee, and Kyung-Suk Suh. Analysis on the characteristics of a pollutant dispersion in river environment. *Annals of Nuclear Energy*, 38(2-3):232–237, 2011.

[16] Carl W Turner and David W Smith. Calcium carbonate scaling kinetics determined from radiotracer experiments with calcium-47. *Industrial & engineering chemistry research*, 37(2):439–448, 1998.

[17] S Sugiharto, Z Su'ud, R Kurniadi, W Wibisono, and Z Abidin. Radiotracer method for residence time distribution study in multiphase flow system. *Applied Radiation and isotopes*, 67(7-8):1445–1448, 2009.

[18] Ryoko Fujiyoshi, Hiroyuki Hirashima, and Sadashi Sawamura. Investigation of the sorption of zn (ii) on surface soils using a radiotracer technique. *Applied radiation and isotopes*, 49(1-2):1–4, 1998.

[19] Marcin Zych, Robert Hanus, Pavel Vlasák, Marek Jaszczur, and Leszek Petryka. Radiometric methods in the measurement of particle-laden flows. *Powder technology*, 318: 491–500, 2017.

[20] Nicholas Tsoulfanidis. *Measurement and detection of radiation*. CRC press, 2010.

[21] Robin Pierce Gardner and Ralph L Ely. *Radioisotope measurement applications in engineering*. Reinhold Publ., 1967.

[22] Glenn F Knoll. *Radiation detection and measurement*. John Wiley & Sons, 2010.

[23] *Application of Radiotracer Techniques for Interwell Studies*. Number 3 in Radiation Technology Series. INTERNATIONAL ATOMIC ENERGY AGENCY, Vienna, 2012. ISBN 978-92-0-125610-2. URL https://www.iaea.org/publications/8658/application-of-radiotracer-techniques-for-interwell-studies.

[24] J Thereska and Z Pang. *Radiotracer Applications in Industry: A Guidebook*. Number 423. IAEA, 2004.

Appendix A

Calibration equations for Detectors

For the Sr-85 radiotracer experiment four NaI detectors were arranged for radiation counting. Before the experiment detectors were calibrated using the three sources of Cs-137, Co-60, Na-22.

The channel-energy calibration equations for detector 1,

$$Energy = 3.055 \times channelno. + 2.920e001 \tag{A.1}$$

The channel- energy calibration equations for detector 2,

$$Energy = 3.614 \times channelno - 5.045 \tag{A.2}$$

The channel- energy calibration equations for detector 3,

$$Energy = 3.480 \times channelno. + 41.76 \tag{A.3}$$

The channel- energy calibration equations for detector 4,

$$Energy = 3.762 \times channelno. - 45.46 \tag{A.4}$$

Appendix B

MCNP model simulation: Input files

B.1 Input file for MCNP model simulation of Na-24 radiotracer experiment

```
c cell cards
 1 1 -11.36 -1 2 -3 4 -5 6 7    $Collimated slab composed of material 1
 2 2  -3.67 -9                  $Detector composed of material 2
 3 3  -3.97 -10                 $Packed bed composed of material 3
 4 0         -8 #1 #2 #3        $Vaccuum inside collimator
 5 0          8                 $Vaccuum in problem boundary


c surface cards
 1 PX 5.08
 2 PX -5.08
 3 PZ 15.24
 4 PZ -15.24
 5 PY 15.24
 6 PY -15.24
 7 RPP -5.08 5.08 -2.54 2.54 -0.635 0.635
```

```
 8 SO 80                                    $Problem boundary
 9 RCC -12.7 0 0 7.62 0 0 7.62              $Detector
 10 RCC 20.63 -15.24 0 0 30.48 0 1.5875     $Packed bed

c Data cards
IMP:P 1 1 1 1 0              $Photons don't matter beyond problem boundary
MODE P                       $Photon transport
SDEF POS=20.63 0 0 ERG=1.3 RAD=D1 AXS=0 1 0 EXT=d2   $Source definition
si1   0 1.5875
sp1 -21 1
si2 -15.24 15.24
sp2 -21 0
F8:P 2
E8 0 1024i 3 $Energy card for different energy bin
M1: 82000 1                      $Natural lead
M2: 11000 1                      $Sodium
     53000 1                     $Iodine
M3: 13000 2                      $Aluminium
     8000 3                      $Oxygen
NPS 10000000 $Number of histories to simulate
```

B.2 Input file for MCNP model simulation of Sr-85 radiotracer experiment

```
    c Detector count rate estimation for volumetric source
c cell cards
 1 1 -11.36 -1 2 -3 4 -5 6 7         $collimated slab composed of material 1
 2 2  -3.67 -9                       $detector composed of material 2
```

```
 3 3  -3.95 -10                      $packed bed composed of material 3
 4 4   -0.001205     -8 #1 #2 #3     $air inside collimator
 5 5   -0.001205     8               $air in problem boundary

c surface cards
 1 PX 2.54
 2 PX -2.54
 3 PZ 5.08
 4 PZ -5.08
 5 PY 5.08
 6 PY -5.08
 7 RPP -2.54 2.54 -1.905 1.905 -0.254 0.254
 8 SO 50                             $problem boundary
 9 RCC  2.54 0 0 7.62 0 0 3.81       $detector
 10 RCC -10.46 0 -1.27 0 0 2.54 1.57 $packed bed

c Data cards
IMP:P 1 1 1 1 0             $photons don't matter beyond problem boundary
MODE P                      $photon transport
c Results are converted to per second per 1 micro Ci
SDEF POS=-10.46 0 0 ERG=0.514 RAD=D1 AXS=0 0 1
     VEC=1 0 0 DIR=D3 EXT=d2 WGT=47306.35          $source definition
si1   0 1.57
sp1 -21 1
si2 -1.27 1.27
sp2 -21 0
si3 0.87 1.0            $Solid angle fraction=0.065 Compensate in WGT card
sp3 0.0 1.0
F8:P 2                  $Energy distribution of pulse created in detector
```

```
E8 0.4 1024i 3          $Energy card for different energy bin
M1: 82000 1                     $Natural lead
M2: 11000 1                     $Sodium
     53000 1                    $Iodine
M3: 17000 0.000415              $Chlorine
     38000 0.000513             $Strontium
     13000 0.528509             $Aluminiam
     08000 0.470563
M4: 7014.42c -0.755             $Nitrogen
     8016.42c -0.232            $oxygen
     18000.42c -0.013           $Argon
M5: 7014.42c -0.755             $Nitrogen
     8016.42c -0.232            $oxygen
     18000.42c -0.013           $Argon
NPS 10000000                    $Number of histories(photons) to simulate
```

Appendix C

Activity and mass calculations for local salt deposits

C.1 Mass calculation for Na-24 salt deposits in Na-24 radiotracer experiment

In the Na-24 radiotracer experiment, the height of the packed bed was 18 inches. The height of each rectangular collimator aperture was 0.5 inches. So, the total packed bed could be considered as a combination of 36 sections with each section of 0.5 inches height. During the experiment, two sections of the packed bed were directly exposed towards two collimator apertures, respectively.

Total activity due to radioactive Na-24 present in the packed bed was $170\mu Ci$. Here,

$$170\mu Ci = 170 \times 37000Bq = 62,90,000Bq = 62,90,000disintegrations/sec$$

Using the equation C.4, the amount of radioactive Na-24 mass equivalent to $62,90,000Bq$,

$$= \frac{62,90,000Bq}{1.29 \times 10^{-5} sec^{-1}} \times \frac{23.991 g/mole}{6.02 \times 10^{23} particles/mole} = 1.94 \times 10^{-11} g$$

So the amount of Na-24 uniformly distributed in each section of the packed bed,

$$= \frac{1.94 \times 10^{-11} g}{36}$$
$$= 5.38 \times 10^{-13} g$$

Corresponding activity from uniformly distributed Na-24 mass at each section,

$$= 174722.222 Bq$$

From the MCNP model, the detector response for each particle simulation,

$$= 0.00015 \pm 0.000003855 counts/particle$$

So, the expected detector response for uniformly distributed activity, R_m,

$$= [(174722 \times 0.00015) \pm (174722 \times 0.000003855)] counts/sec$$
$$= 26.21 \pm 0.67 counts/sec$$

Now,

$$\frac{M_t}{R_t} = \frac{M_m}{R_m}$$

where,

M_t = Local mass deposition of salt in the test section

M_m = Mass of salt uniformly deposited through test section = $5.38 \times 10^{-13} g$

R_m = Detector Response for local uniform activity = $26.21 counts/sec$

R_t = Detector Response for local activity in test section

At saturation,

$$R_t = 910.875 counts/sec$$

Considering 40% void fraction in packed bed, local mass of Na-24 salt deposition in packed bed at saturation near detector-1,

$$M_t = 910.875 counts/sec \times 0.40 \times \frac{5.38 \times 10^{-13} g}{26.21 counts/sec} = 7.41 \times 10^{-12} g = 7.41 pg$$

C.2 Activity calculation for locally deposited Sr-85 salt

Experimental and MCNP simulation data for detector response		
Detector	Average counts/sec from experiment at saturation	Counts/sec per activity concentration from MCNP simulation
1	599	433 ± 1.33
2	107	446 ± 1.36
4	54	449 ± 1.36

Table C.1: Detector response data from Sr-85 radiotracer experiment

In the Sr-85 radiotracer experiment, the detector response, R_t, recorded for detector-1 was $599 counts/sec$. From the MCNP simulation, the detector response, R_m, estimated for detector-1 was $433 counts/sec$. The total amount of activity present in the MCNP domain, A_m, was $19.67 \mu Ci$. The table C.1 contains experimental and MCNP simulated detector responses for detector-1, detector-2 and detector-4. Using the relation 5.1, the local activity of the deposited Sr-85 corresponding to the detector-1 counting data was calculated in the following manner,

$$A_t = \frac{R_t}{R_m} \times A_m \tag{C.1}$$

$$A_t = \frac{599}{433} \times 19.67 = 27.21 \mu Ci$$

Similarly, the calculated local activities corresponding to the detector-2 and detector-4 radiation responses were $4.72 \mu Ci$ and $2.36 \mu Ci$.

C.3 Mass calculation for the locally deposited Sr-85 salt

Mass of radioactive materials can be estimated from activity using the equation 5.3. This equation can be rewritten as follows,

$$N = \frac{A}{\lambda} \tag{C.2}$$

From the number of radioactive particles, N, total mass of radioactive particles, m, can be determined using the following relationship,

$$m = N \times \frac{1\text{mole}}{N_A} \times \frac{M}{1\text{mole}} \tag{C.3}$$

$$m = \frac{A}{\lambda} \times \frac{1\text{mole}}{N_A} \times \frac{M}{1\text{mole}} \tag{C.4}$$

Here, m is the mass of radioisotopes, N is the total number of particles, N_A is the

Avogadro number, M is the atomic weight of the radioisotope, A is the activity in Bq or disintegrations/sec and λ is the decay constant of the radioisotope.

For the activity of $27.21\mu Ci$ of Sr-85 radioisotopes, corresponding radioactive mass,

$$m = \frac{27.21 \times 37000Bq}{1.24 \times 10^{-7}sec^{-1}} \times \frac{1\text{mole}}{6.02 \times 10^{23}particles} \times \frac{84.9g}{1\text{mole}}$$

$$m = 1.15 \times 10^{-9}g = 1145.08pg$$

Considering 40% void fraction in the packed bed, the amount of locally deposited Sr-85,

$$m = 0.40 \times 1145.08pg = 458.032pg$$

Similarly, Sr-85 deposited mass corresponding to $4.72\mu Ci$ and $2.36\mu Ci$ are $79.54pg$ and $39.82pg$, respectively.

Appendix D

Uncertainty calculation

D.1 Uncertainty calculation for deposited salt mass in Na-24 radiotracer experiment

From the Na-24 radiotracer experiment, the amount of deposited Na-24 mass was estimated $7.41pg$. The Na-24 mass deposit, M_t was calculated using the following equation,

$$M_t = \frac{R_t}{R_m} \times M_m \times 0.40$$

where,

M_t = Local mass deposition of salt in the test section

M_m = Mass of salt uniformly deposited through test section = $5.38 \times 10^{-13} g = 0.538pg$

R_m = Detector Response for local uniform activity = $26.21 \pm 0.67 counts/sec$

R_t = Detector Response for local activity in test section = $910.875 \pm 9.544 counts/sec$

The multiplication factor 0.40 in equation came from the 40% void fraction of the packed bed.

Experimental data for uncertainty calculation of Na-24 mass deposit	
Total average counts at saturation of Na-24 mass deposition, A_i	$9108.75 counts$
Radiation counting time, t	$10 sec$
Count rate at saturation of Na-24 mass deposition	$910.875 counts/sec$

Table D.1: Top detector response data from Na-24 radiotracer experiment

Uncertainty in R_t was calculated as follows,

$$\sigma_{R_t} = \frac{\sqrt{A_i}}{t} = \frac{\sqrt{9108.75}}{10} = \pm 9.544 counts/sec$$

Detector response for local uniform activity, R_m, was calculated from the Na-24 activity uniformly distributed in each section of packed bed and the MCNP simulated detector response for each particle simulation. Uniformly distributed Na-24 activity in each section of packed bed was $174722.222 Bq$. Detector response per particle simulation from MCNP simulation was $0.00015 \pm 0.000003855 counts/particle$.

MCNP simulation data for uncertainty calculation of Na-24 mass deposit	
Detector response per particle simulation	$0.00015 \pm 0.000003855 counts/particle$
Count rate for uniformly distributed activity at each section	$26.21 \pm 0.67 counts/sec$

Table D.2: Detector response data from MCNP simulation

R_m was calculated as,

$$R_m = 174722.222 \times 0.00015 counts/sec = 26.21 counts/sec$$

The uncertainty of a function f(x) of a single variable x with uncertainty σ_x is calculated

using the following expression,

$$\sigma_f = \mid \frac{df}{dx} \mid \times \sigma_x \tag{D.1}$$

Using the above relation, uncertainty in R_m was calculated as,

$$\sigma_{R_m} = 174722.222 \times 0.000003855 counts/sec = \pm 0.67 counts/sec$$

From the law of propagation of errors, for a function f of two variables x and y with corresponding uncertainties σ_x and σ_y, the uncertainty in $f(x, y)$ is estimated in the following manner if the measurements of x and y are uncorrelated,

$$\sigma_f = \sqrt{\left[\frac{\partial f}{\partial x}\right]^2 \sigma_x^2 + \left[\frac{\partial f}{\partial y}\right]^2 \sigma_y^2} \tag{D.2}$$

Using the above equation, the uncertainty for M_t was calculated from the uncertainties of R_t and R_m as follows,

$$\sigma_{M_t = 0.40 \times \sqrt{\left(\frac{M_m}{R_m}\right)^2 \sigma_{R_t}^2 + \left(\frac{R_t M_m}{R_m^2}\right)^2 \sigma_{R_m}^2}}$$

$$\sigma_{M_t = 0.40 \times \sqrt{\left(\frac{0.538}{26.21}\right)^2 \times (9.544)^2 + \left(\frac{910.875 \times 0.538}{(26.21)^2}\right)^2 \times (0.67)^2}}$$

$$\sigma_{M_t} = \pm 0.21 pg$$

D.2 Uncertainty calculation for local activity in Sr-85 radiotracer experiment

At saturation of Sr-85 mass deposition, average corresponding count rates recorded for detector-1, detector-2 and detector-4 were $599 counts/sec$, $107 counts/sec$ and $54 counts/sec$, respectively. The LLD set at $494 keV$, $443 keV$ and $424 keV$ for detector-1, detector-2 and detector-4, respectively. From MCNP simulation, the corresponding detector responses for detector-1, detector-2 and detector-4 were $433 \pm 1.33 counts/sec$, $446 \pm 1.36 counts/sec$,

$449 \pm 1.36 counts/sec$. The amount of activity present in the MCNP domain, A_m, $19.67 \mu Ci$. Now, for detector-1,

$$R_t = 599 counts/sec$$

$$R_m = 433 counts/sec$$

$$\sigma_{R_t} = \sqrt{599} counts/sec = 24.47 counts/sec$$

$$\sigma_{R_m} = 1.33 counts/sec$$

$$A_t = 27.21 \mu Ci$$

Local activity deposited in packed bed near detector-1 was $27.21 \mu Ci$. So, using the law of propagation of errors, equation D.2, explained in the previous section, the uncertainty in local activity of the test section near detector-1 was estimated,

$$\sigma_{A_t = \sqrt{(\frac{A_m}{R_m})^2 \sigma_{R_t}^2 + (\frac{R_t \times A_m}{R_m^2})^2 \sigma_{R_m}^2}}$$

$$\sigma_{A_t = A_m \sqrt{(\frac{1}{R_m})^2 \sigma_{R_t}^2 + (\frac{R_t}{R_m^2})^2 \sigma_{R_m}^2}}$$

$$\sigma_{A_t = 19.67 \sqrt{(\frac{1}{433})^2 \sigma_{24.47}^2 + (\frac{599}{433^2})^2 \sigma_{1.33}^2}}$$

$$\sigma_{A_t} = \pm 1.11 \mu Ci$$

Similarly, the uncertainties for local activities near detector-2 and detector-4 were estimated $0.45 \mu Ci$ and $0.32 \mu Ci$.

D.3 Uncertainty calculation for the mass of Sr-85 deposits in Sr-85 radiotracer experiment

Atomic weight of Sr-85 $= 84.9g$

Avogadro number, $N_A = 6.02 \times 10^{23} particles/mole$

Decay constant for Sr-85 radioisotope $= 1.24 \times 10^{-7} sec^{-1}$

Multiplication factor due to 40% void fraction in packed bed $= 0.40$

Uncertainty in Sr-85 local activity near detector-1 $= \pm 1.11 \mu Ci = \pm 41070 Bq$

So, using equation D.1, uncertainty in local Sr-85 mass deposits near detector-1,

$$\sigma_{M_t} = 0.40 \times \frac{\pm 41070}{1.24 \times 10^{-7}} \times \frac{84.9}{6.02 \times 10^{23}} = \pm 1.868 \times 10^{-11} g = \pm 18.68 pg$$

Similarly, the uncertainties in Sr-85 local mass deposits near,

Detector 2 $= \pm 7.68 pg$

Detector 4 $= \pm 5.4 pg$